

Project Report: 15E612 Innovation Practices Laboratory

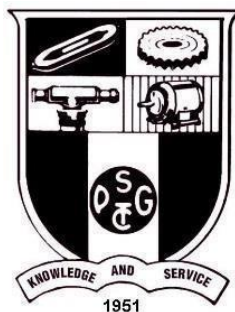
Title: SYNRM PERFORMANCE ANALYSIS

| NAME | ROLL NO |
|------------------|---------|
| SAKTHIVEL C | 18E637 |
| SARAVANA KUMAR V | 18E640 |
| SHANKAR R | 18E641 |

Project report for 15E612 INNOVATION PRACTICES LABORATORY

BACHELOR OF ENGINEERING

Branch: **ELECTRICAL AND ELECTRONICS ENGINEERING
(SANDWICH)**



NOV 2021

**DEPARTMENT OF ELECTRICAL AND ELECTRONICS
ENGINEERING**

PSG COLLEGE OF TECHNOLOGY

(Autonomous Institution)

COIMBATORE – 641 004

PSG COLLEGE OF TECHNOLOGY

(Autonomous Institution)

COIMBATORE – 641 004

SYNRM PERFORMANCE ANALYSIS

Bona fide record of work done by

| NAME | ROLL NO |
|------------------|---------|
| SAKTHIVEL C | 18E637 |
| SARAVANA KUMAR V | 18E640 |
| SHANKAR R | 18E641 |

Dissertation submitted in partial fulfillment of the requirements for the degree
of

BACHELOR OF ENGINEERING

**Branch: ELECTRICAL AND ELECTRONICS ENGINEERING
(SANDWICH)**

of ANNA University

NOVEMBER 2021



Dr. Balaji V

Faculty guide

Dr. Kanakaraj J

Head of the Department

Certified that the candidate was examined in the viva-voce examination
held on

(Internal Examiner)

(External Examiner)

ACKNOWLEDGEMENT

We express our sincere thanks to **Dr. K. Prakasan**, Principal-In charge, PSG College of Technology for providing the necessary support during this difficult time.

We extend our gratitude to **Dr. J. Kanakaraj**, Professor and Head of the Department of Electrical and Electronics Engineering, who has encouraged us to come with new ideas towards the betterment of the future.

Our sincere thanks to our Innovation Practices faculties **Dr. A. Soundarajan**, Professor and Program Co-Ordinator of Department of Electrical and Electronics Engineering, **Dr. B. Sathy**a, Assistant Professor (Sr. Gr.), **Mr. N. Sampathraja** Assistant Professor (Sr. Gr.), Department of Electrical and Electronics Engineering, for providing us valuable inputs and supporting us throughout the work.

We thank **Dr. V. Balaji**, Assistant Professor, Department of Electrical and Electronics Engineering, our Project Guide and one of the inspirations to carry on our project. We have learnt many things from you sir not only in academics but also in practical view. And once again we thank you, sir. Without your knowledge, we might not finish our project.

We sincerely thank **Dr. A. Soundarajan**, Professor and Program Co-Ordinator of Department of Electrical and Electronics Engineering for providing constant support.

We thank our Tutor, **Dr. B. Sathy**a, Assistant Professor, Department of Electrical and Electronics Engineering, for the guidance and for motivating us to complete the project. Thank you, sir.

We also express our sincere gratitude towards **Mr. P. Varunraj**, Senior Research Fellow, Department of Robotics and Automation Engineering, for helping us to understand the concept behind the Design of SynRM and providing us absolute knowledge.

We thank and also dedicate this project to all the members of the faculty of the Department of Electrical and Electronics Engineering, PSG College of Technology and our classmates, for providing constant support and motivation. Thank you all.

TABLE OF CONTENT

| | |
|---|-----------|
| 1. INTRODUCTION | 1 |
| 1.1 RARE-EARTH MAGNET PRICE VOLATILITY | 1 |
| 1.2 HISTORICAL PERSPECTIVES ON SYNCHRONOUS MACHINES AND DRIVES | 3 |
| 1.2.1 PM SYNCHRONOUS MACHINE | 3 |
| 1.2.2 SYNCHRONOUS RELUCTANCE MACHINES..... | 5 |
| 1.2.3 PMSM TO SYNCHRONOUS RELUCTANCE MACHINE..... | 8 |
| 2. LITERATURE SURVEY..... | 9 |
| 2.1 INDEXED JOURNALS | 9 |
| 3. INDUCTION MOTOR..... | 12 |
| 3.1 HISTORY AND DEVELOPMENT | 12 |
| 3.2 WORKING PRINCIPLE | 12 |
| 3.3 STATOR DESIGN | 14 |
| 3.3.1 CALCULATION | 15 |
| 3.4 ROTOR DESIGN | 16 |
| 3.5 GEOMETRY DATA | 17 |
| 3.6 SIMULATION RESULTS..... | 18 |
| 3.7 LOSS DISTRIBUTION | 21 |
| 4. SYNCHRONOUS RELUCTANCE MACHINE | 23 |
| 4.1 INTRODUCTION | 23 |
| 4.2 SYNCHRONOUS RELUCTANCE MOTOR | 24 |
| 4.3 WORKING..... | 24 |
| 4.4 PERFORMANCE | 26 |
| 5. IMPLEMENTATION OF 3 FLUX BARRIER MODEL | 27 |
| 5.1 INTRODUCTION | 27 |
| 5.2 SYNRM GEOMETRY FOR 3 FLUX BARRIERS | 27 |
| 5.3 DESIGN PARAMETERS | 28 |
| 5.4 SYNRM GEOMETRY - AXIAL VIEW | 29 |
| 5.5 WINDING | 30 |
| 5.6 3D MODEL OF SYNRM | 31 |
| 5.7 MATERIALS USED FOR STATOR AND ROTOR DESIGN | 31 |
| 5.8 INPUT PARAMETERS..... | 32 |
| 5.9 OUTPUT..... | 34 |
| 5.10 GRAPHS | 34 |

| | |
|--|----|
| 5.11 TORQUE RIPPLE | 35 |
| 5.12 E-MAGNETICS | 36 |
| 6. MODELLING AND IMPLEMENTATION OF 4 FLUX BARRIER SYNRM | 37 |
| 6.1 INTRODUCTION | 37 |
| 6.2 SYNRM MODEL WITH 4 FLUX BARRIERS | 37 |
| 6.3 AXIAL VIEW OF SYNRM | 38 |
| 6.4 3-D MODEL OF SYNRM | 38 |
| 6.5 WINDING | 39 |
| 6.6 INPUT PARAMETERS..... | 40 |
| 6.7 MATERIALS USED..... | 40 |
| 6.8 OUTPUT..... | 41 |
| 6.8.1 TORQUE RIPPLE..... | 41 |
| 6.9 GRAPHS..... | 42 |
| 6.10 E -MAGNETICS | 43 |
| 7. ANALYSIS AND VERIFICATION | 44 |
| 7.1 ROTOR DESIGN CHARACTERISTICS | 44 |
| 7.2 SALIENCY RATIO | 44 |
| 7.3 SYNRM WITH 1 AND 2 FLUX BARRIERS | 45 |
| 7.4 OUTPUT AND INFERENCE..... | 46 |
| 7.5 MULTILAYER BARRIER MODEL..... | 47 |
| 7.6 RESULTS IN 3 AND 4 BARRIER MODEL..... | 48 |
| 7.7 NEED FOR FLUX BARRIERS AND CARRIERS | 48 |
| 7.8 RELATION BETWEEN POWER FACTOR AND NO OF FLUX BARRIERS | 49 |
| 7.9 RELATION BETWEEN SALIENCY RATIO AND NO OF FLUX BARRIERS | 49 |
| 7.10 REALTION BETWEEN SALIENCY RATIO AND POWER FACTOR | 50 |
| 7.11 RELATION TO ACHIEVE MAXMIMUM POWER FACTOR | 50 |
| 7.12 RESULTS FOR 3 FLUX BARRIER MODEL | 51 |
| 7.13 TO ACHIEVE MAXIMUM POWER FACTOR | 52 |
| 7.14 RESULTS OBTAINED FOR 4 FLUX BARRIER MODEL..... | 52 |
| 8. COMPARISON BETWEEN IM AND SYNRM | 55 |
| 9. CONCLUSION..... | 56 |
| 9.1 SUMMARY OF WORK DONE..... | 56 |
| 9.2 FUTURE WORK..... | 56 |
| BIBLIOGRAPHY:..... | 57 |

LIST OF FIGURES

| | |
|--|----|
| Figure 1: Rare Earth Magnet Price..... | 2 |
| Figure 2: PMSM with Alnico | 3 |
| Figure 3: PMSM Rotor Component | 4 |
| Figure 4: IPM Machine using ferrites..... | 5 |
| Figure 5: Cross section view of basic 2-pole synchronous machine with circumferential segments | 6 |
| Figure 6: Sketch of 4-pole SynRM rotor with 7 flux barriers per pole | 7 |
| Figure 7: 4-pole axially laminated syn machine with four C-core quadrants | 7 |
| Figure 8: Torque speed curve for a typical IM with quadratic load torque..... | 13 |
| Figure 9: Squirrel cage induction motor..... | 13 |
| Figure 10: Name plate details of 90L framed induction machine | 14 |
| Figure 11: Typical squirrel cage with skew and end rings at both ends | 16 |
| Figure 12: Geometry Data for Stator and Rotor..... | 17 |
| Figure 13: Efficiency vs Speed..... | 19 |
| Figure 14: power factor vs Speed..... | 19 |
| Figure 15: Torque vs Speed..... | 20 |
| Figure 16: Power vs Speed | 20 |
| Figure 17: On load Iron loss | 21 |
| Figure 18: stator copper loss | 21 |
| Figure 19: Typical loss distribution for an induction motor | 22 |
| Figure 20: SynRM Rotor | 23 |
| Figure 21: Sketch of a synchronous reluctance motor with..... | 24 |
| Figure 22: Cross sectional view of SynRM motor | 25 |
| Figure 23: SynRM Stator and Rotor Geometry | 27 |
| Figure 24: SynRM Model with 3 flux barriers | 29 |
| Figure 25: Axial View | 29 |
| Figure 26: Winding pattern | 30 |
| Figure 27: 3D Model of SynRM | 31 |
| Figure 28: Materials Chosen for Stator and Rotor | 32 |
| Figure 29: Name plate details | 33 |
| Figure 30: Input Details | 33 |
| Figure 31: Output Data Obtained for 3 Flux Barrier Model | 34 |
| Figure 32: Torque vs Speed..... | 34 |
| Figure 33: Torque vs Position | 35 |
| Figure 34:E-Magnetics for 3 Flux Barrier Model | 36 |
| Figure 35: SynRM 4 Flux Barrier Model | 37 |
| Figure 36:Axial view 4 Layer Barrier Model | 38 |
| Figure 37: 3D model of 4 Layer Barrier Model..... | 38 |
| Figure 38: Winding Pattern | 39 |
| Figure 39: Input Details | 40 |
| Figure 40: Materials used for Stator and Rotor..... | 40 |
| Figure 41: Output Data for 4 Layer Flux Barrier Model | 41 |
| Figure 42: Torque vs Position | 42 |

| | |
|--|----|
| Figure 43: Torque vs Speed..... | 43 |
| Figure 44: E-Magnetics for 4 Flux Barrier Model | 43 |
| Figure 45: D and Q Axis..... | 45 |
| Figure 46: SynRM with 1 flux barrier | 45 |
| Figure 47: SynRM with 2 flux barrier | 45 |
| Figure 48: Multilayer Barrier Model | 47 |
| Figure 49: Power factor vs No. of Flux Barriers | 49 |
| Figure 50: Saliency ratio vs No. of Flux Barriers..... | 49 |
| Figure 51: Saliency ratio vs Current angle..... | 51 |
| Figure 52: power factor vs current angle | 51 |
| Figure 53: Torque ripple vs Current angle | 52 |
| Figure 54: power factor vs current angle | 53 |
| Figure 55: Torque vs Current angle..... | 53 |
| Figure 56: saliency ratio vs current angle | 54 |

LIST OF TABLES

| | |
|---|----|
| Table 1: Stator Geometry Data | 18 |
| Table 2: Rotor Geometry Data | 18 |
| Table 3: Simulation output data..... | 19 |
| Table 4: Saliency Ratio | 46 |
| Table 5: Saliency Ratio for 4 flux barrier..... | 48 |
| Table 6: Comparison between IM and SynRM | 55 |

SYNOPSIS

The Permanent magnet (PM) Synchronous motors are more attractive when it comes to Electric vehicle market. The main advantages this motor offers is high power density and high reliability design. The PMSM Is relatively easy to control and it exhibits excellent performance in terms of maximum torque per ampere control and good speed operation.

The PMSM are classified based on the position of permanent magnets and are classified as surface or interior mounted permanent magnets. This usage of magnets makes the cost of raw materials required for the manufacture of PMSM makes it uncertain in the long run. Also, PMSM motor also has certain technical disadvantages that limit the performance in particular the demagnetisation effect that if temperature of motor exceeds its operating conditions.

Therefore, there is a growing attention in alternative solutions that include rare (RE) earth free machines such as Synchronous Reluctance motors.

Our project focuses on this SynRM's performance characteristics (torque characteristics) and power factor analysis.

PROBLEM STATEMENT

SynRM provides high efficiency even though its power factor is low. In order to replace PMSM many companies are working on Manufacturing IE5 Efficiency rated SynRM with better performance.

PROBLEM SOLUTION

In this Project we mainly focus on modelling a 3 phase 4 pole 2.2kW 3000 rpm rated SynRM for industrial applications. As a part the induction motor with same rating was modelled first. In order to reduce cost many companies use Induction motor's Stator for SynRM. The induction motor was designed for same rating after that its stator part design was kept fixed and rotor design alone was changed to model SynRM. 4 different models of SynRM rotor was modelled and analysed which produces better torque characteristics and high power factor.

OBJECTIVES

The objective of the project is to design SynRM and Induction machines for ratings collected from Danfoss lab, PSG college of technology. The objectives are.

1. To model Induction motor and Synchronous reluctance motor for the nameplate specs.
2. To model SynRM with 4 different rotor characteristics and to analyse the model which produces lower torque ripple and high power factor.

TECHNOLOGIES USED

The software used for this project is Ansys MotorCad. It is a machine design tool with fast Multiphysics simulation over a wide torque speed operating range. The Induction machine and SynRm were modelled using this software.

ABSTRACT

This project focuses on the key notions about analysis and design of synchronous reluctance motors. The aim is to highlight not only the advantages of such machines but also some drawbacks such as the low power factor and the torque ripple. The strategies to reduce such drawbacks are also reported with mathematical justification. Some tricks to overcome the torque ripple are described.

1

INTRODUCTION

Many veteran professionals in the PM synchronous machine industry will never forget the severe stress they suffered during the period from early 2010 to mid-2011. When the price of the rare-earth metal neodymium (Nd) skyrocketed on the world market by a factor greater than 20:1. This unprecedented price increase was extremely painful for even large companies that were heavily dependent on neodymium as a key ingredient in their high-strength rare-earth magnets, and it forced some smaller companies without the necessary financial resources to go out of business.

As a result, there has been a dramatic surge of activities during the period since 2010 to investigate the viability of developing alternative types of machines that would provide comparably high performance without being so exposed to the volatility of future price swings for the neodymium-iron-boron (NdFeB) magnets. Some researchers have pursued alternative types of synchronous machines in search of the best candidates. Others have instead investigated entirely different types of brushless machines including high performance versions of switched reluctance and induction machines.

1.1 RARE-EARTH MAGNET PRICE VOLATILITY

The commercialization of NdFeB rare-earth permanent magnets that began in the 1980s has had a profound effect on the successful development of high-performance PM synchronous machines that have appeared in so many important applications during recent years ranging from passenger electric vehicles to elevators and wind turbines. Despite their many attractive performance characteristics, NdFeB magnets suffer from a relatively low Curie temperature that puts them at a disadvantage compared to other types of magnets, including samarium-cobalt magnets, for use in demanding electric machine applications that often push the thermal limits of their wire insulation systems.

Material scientists soon learned that one of the most effective means of increasing the maximum temperature range of NdFeB

magnet is to add small amounts another rare-earth element, dysprosium (Dy). Despite of having maximum operating temperature, the impact of adding dysprosium on magnet cost becomes increasing significant as its percentage content grows because Dy is significantly rarer and more expensive than Nd. In fact, the cost per kilogram of dysprosium is typically on the order of 7 to 8 times more expensive than Nd, signifying that even small percentages of Dy in the NdFeB magnets will have a significant impact on the cost of the final magnet material.

Although the price of NdFeB magnets was initially quite high, China played a major role in driving down their price during the late 1990s and early 2000s. China was in a strong position to play such an important role in the NdFeB magnet market because of its very large reserves of rare-earth materials compared to any other country. During this time period, Chinese magnet producers became the dominant NdFeB magnet manufacturers in the world.

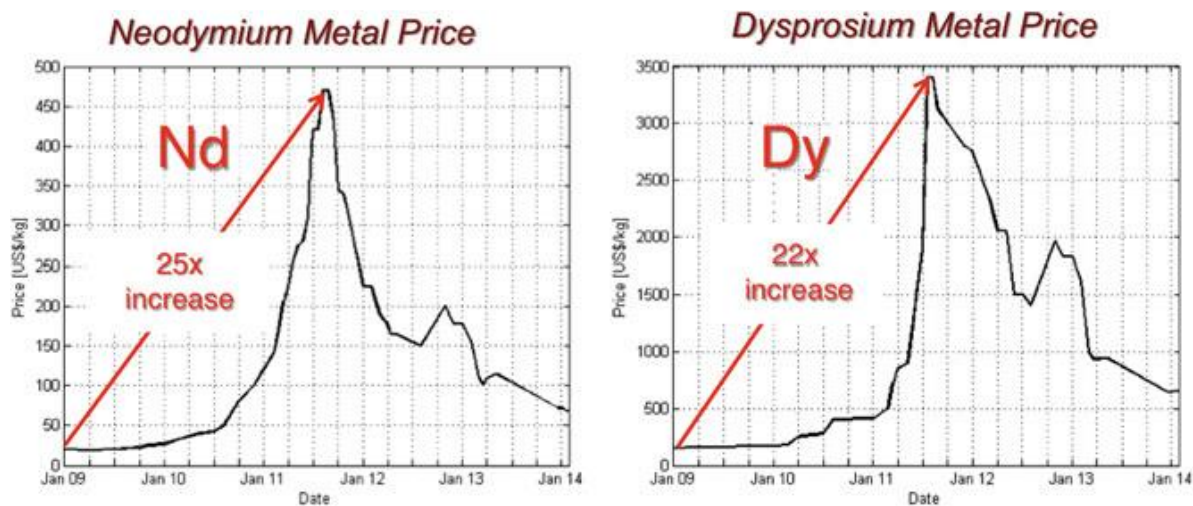


Figure 1: Rare Earth Magnet Price

This figure shows that the prices per kg for neodymium and dysprosium increased in tandem between the beginning of 2010 and mid-2011 by factors of 25 and 22 times, respectively, due to a combination of factors that included a large component of market speculation. After hitting their peak, prices of both materials dropped almost as rapidly and have settled to values that approach their pre bubble prices. As noted in the introduction, this spectacular increase has had a major financial and psychological effect on PM machine manufacturers that had become increasingly

dependent on both of these materials as the basis for the growing amount of magnet material that they needed to build their PM machines.

1.2 HISTORICAL PERSPECTIVES ON SYNCHRONOUS MACHINES AND DRIVES

1.2.1 PM SYNCHRONOUS MACHINE

Although the concept of mounting permanent magnets on spinning rotors to produce electric motors and generators predates the 20th century, the commercial implementation of PM synchronous machines had to await the development of magnet materials with sufficient remanent flux density and coercivity to make them practical. The availability of high-grade Alnico magnets also led to development and commercialization of some of the earliest examples of line-start PM synchronous machines, representing the hybridization of induction and synchronous machine features in the same rotor.

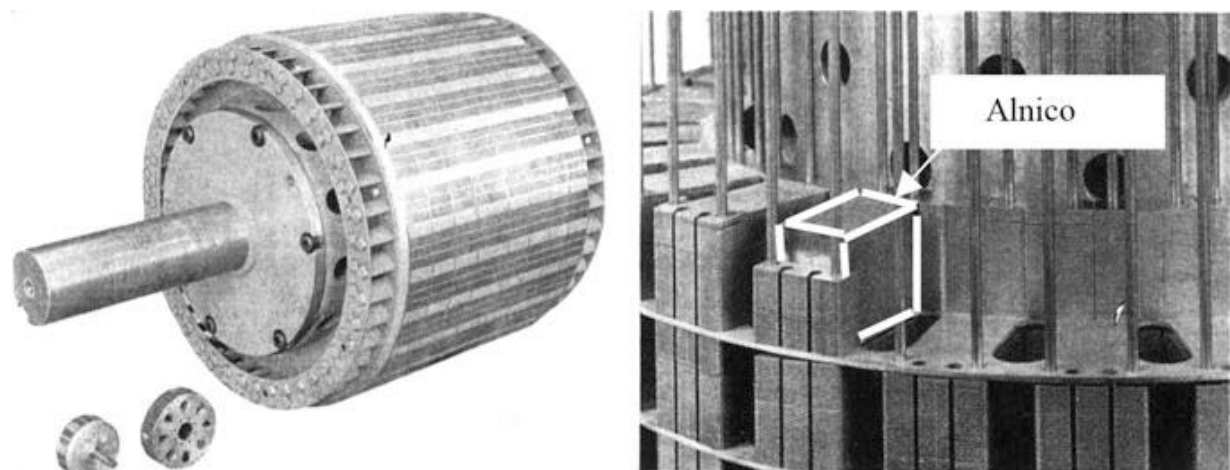


Figure 2: PMSM with Alnico

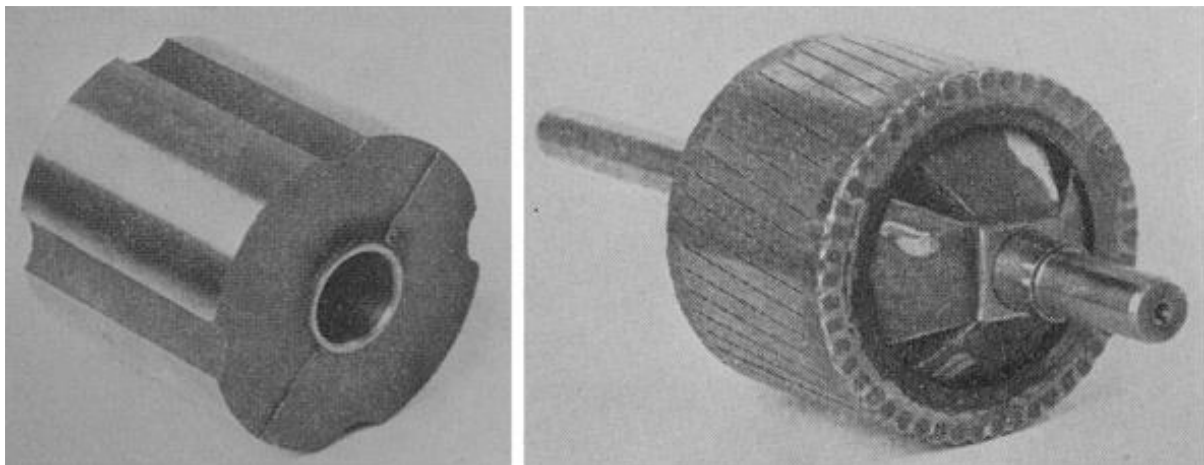


Figure 3: PMSM Rotor Component

Rotor components of the Permasyn family of line-start PM synchronous machines designed with: **Left** Alnico magnets at the core of the motor and **Right** Fully-assembled line-start rotor showing the details of the squirrel cage at the outer periphery of the rotor.

Ferrite ceramic permanent magnets first became commercially available in the 1960s as a lower-cost alternative to metallic magnets. The low cost of ferrite magnets combined with their other attractive features, including excellent corrosion resistance, has led to their tremendous commercial success. Ferrite magnets became appealing candidates for use in PM synchronous machines very soon after the magnet material became available over 50 years ago. They have been successfully applied in a wide variety of PM machine topologies including both surface and interior magnet configurations.

Although PM machines using ferrite magnets cannot compete with designs using newer grades of sintered rare-earth magnets in applications that require the highest possible torque/power density, the use of ferrite magnets continues to draw attention from machine designers today because of their wide availability and low cost. The opportunity to extract significant amounts of reluctance torque from interior PM machines in addition to the magnet torque became more widely recognized in the 1970s.

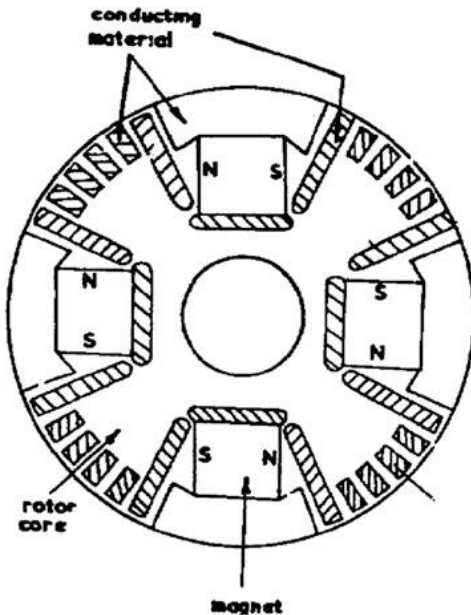


Figure 4: IPM Machine using ferrites

The commercial availability of high-strength rare-earth magnets, beginning with Samarium-Cobalt (SmCo) magnets in the 1970s, followed by Neodymium-Iron-Boron (NdFeB) magnets in the 1980s, made it possible to achieve significantly higher values of torque-and power density with PM synchronous machines. For several years after the introduction of these rare-earth magnets, their applications in high-performance PM synchronous machine drives were limited to specialty applications such as servo drives for machine tools and robotics because of the high cost of the magnets. Magnet manufacturers located in China, taking advantage of China's large deposits of rare-earth minerals, gradually succeeded in driving down the cost of NdFeB magnets during the 1990s, opening the door to the much wider applications of high-performance PM machine drives in a variety of cost-sensitive applications.

1.2.2 SYNCHRONOUS RELUCTANCE MACHINES

While PM synchronous machines have attracted significant attention from researchers since the 1980s for high-performance drive applications, there was also interest in the development of synchronous reluctance machines that did not require magnets or any field excitation at all. Commercial interest in the development of synchronous reluctance machines for adjustable-speed drive applications grew in the 1960s and 1970s as solid-state inverter

technology matured. These machines were popular choices for textile mill process line applications where several of these machines could be operated in exact synchronism if they were excited in parallel by the same inverter. A type of synchronous reluctance machine that was developed in the 1960s using circumferential segments of lamination steel with copper cage bars between adjacent segments

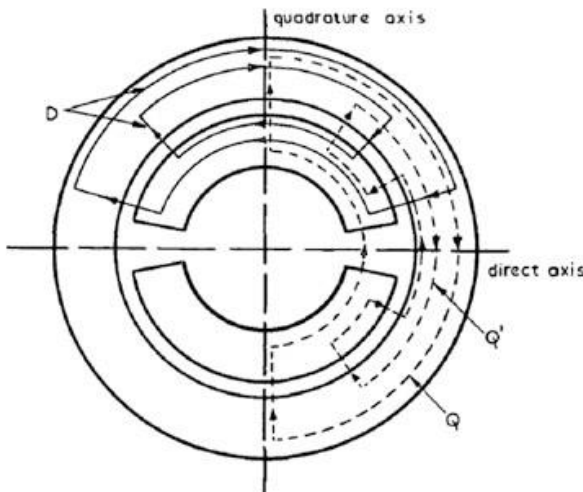


Figure 5: Cross section view of basic 2-pole synchronous machine with circumferential segments

It was recognized by Kostko in 1923 that the performance of the synchronous reluctance machines would be quite poor in terms of efficiency and power factor unless the machine is designed to achieve a high magnetic saliency. His solution was to break the rotor into multiple sections that served as flux guides to increase the difference between the inductances along the d and q-axes. During subsequent years, this concept evolved, leading to increasingly sophisticated design guidelines and implementations intended for adjustable-frequency drive configurations.

One intriguing technique for increasing the magnetic saliency in synchronous reluctance machines above the levels achievable with conventionally-laminated machine is to, instead, laminate the machine in the axial direction using nested strips of grain-oriented lamination steel that are separated by thin layers of insulating material.

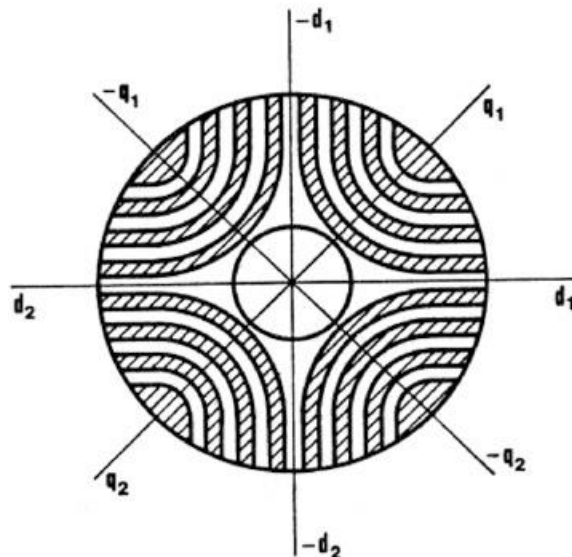


Figure 6: Sketch of 4-pole SynRM rotor with 7 flux barriers per pole

The most appealing feature of this axially-laminated rotor construction is the opportunity to significantly increase the number of flux barriers per pole, making it possible to provide a major boost to the machine's magnetic saliency. This elevated saliency which in turn increases the machine's power factor and potentially, its efficiency as well by lowering the required stator current.

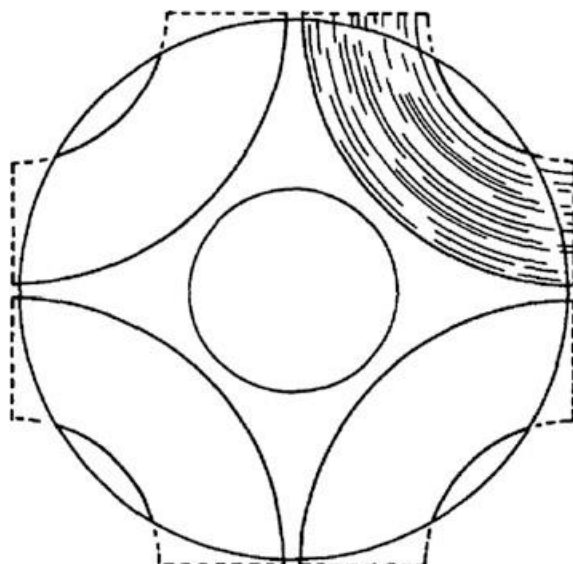


Figure 7: 4-pole axially laminated syn machine with four C-core quadrants

Unfortunately, the axially laminated construction is vulnerable to elevated iron losses in the rotor laminations close to the air gap, limiting its efficiency advantages. Perhaps even more importantly, the significant manufacturability challenges associated with this

axially laminated rotor constructions have seriously hindered its commercialization opportunities.

1.2.3 PMSM TO SYNCHRONOUS RELUCTANCE MACHINE

Because of the several advantages we likely move to Synchronous Reluctance Machine than PMSM. The cost is also plays a major role in transferring to SynRM. In present, many industries and companies are moving towards SynRM for its good efficiency and power factor in low cost.

2

LITERATURE SURVEY

2.1 INDEXED JOURNALS

1. Duc-Kien-Ngo and Min-Fu-Hsieh et al [1], have compared two different catagories of permanent magnet layouts for performance improvements and electromagnetic characteristics. Analysis on permanent magnet arrangement position and how it improves the torque production and methods to overcome irreversible demagnetization have been inferred.
2. Hui Yu, Xinxing Zhang, Jinghua Ji and Liang Xu et al [2], have suggested a new rotor design for synchronous reluctance motor for improved torque characteristics. the motor parameters are optimized using finite element analysis. Compared with Normal SynRM's the torque ripple of the optimized rotor was reduced to around 83.5% based on constant average torque. this methodology suggested improves motor efficiency to around 86% which achieve design requirements for SynRM.
3. S Tahi, R Ibtiouen, M Boumekhla et al [3], produced an optimization method based on cyclic coordination method coupled with FEM has been applied successfully for the design of synchronous reluctance machine structures for the design of SynRM with a massive rotro and with a flux barrier rotor for given stator conditions. Thereby optimizing the output torque and power factor.
4. Alireza Siadatan, Jacob Goltieb et al [4], Ebrahim Afjei have designed a SynRM with four obstacles and eight pieces of magnet. Location of the magnets in the obstacle and the dimensions of flood barrier has a potential ramp of the PmSynRM torque structure.

5. Nezih Gokhan Ozcelik, Ugur Emre Dogru, Murat Imeryuz and Lale T Ergene et al [5], have modelled three different induction motor models with (2.2kW,4kW,5.5kW) and compared with Synchronous reluctance motor with different no of flux barriers and rotor structure. They have concluded that the SynRM has higher efficiency than induction machine and rotor losses were also eliminated in SynRM.
6. Sibasish Panda, Ritesh Kumar Keshri et al [6], are try to explore the feasibility of non-permanent magnet by considering the design and analysis of 1.5kW Synchronous Reluctance Motor (SynRM). They verified and optimized the data through Finite Element Method (FEM) analysis. They conclude that the rotor structure is plays a vital role to get improved torque performance specifically torque ripple and average torque.
7. Andre Nasr, Baptiste Chareyron, Abdelli Abdenour and Misa Milosavljevic et al [7], have proposed alternative for NdFeB using Ferrite magnets due to its low cost. They used more ferrite magnets to increase the performance and to reduce the torque ripples.
8. Gianmario Pellegrino, Thomas N. Jahns, Nicola Bianchi, Wen L. Soong, Francesco Cupertino et al [8], have proposed that the Synchronous Reluctance Motors as an more advantages compared to all motors and get more efficiency when ferrite permanent magnets are used. They undergo several factors and conclude that SynRM brings major impact in the field.
9. Olexiy Iegorov, Olga Iegorova, Mykolay Kundenko and Natalia Potryvaieva et al [9], have modelled four different rotor structure types with common stator structure type and analysed through simulation computer simulation methods. They conclude that at low pulsations of torque it will obtain high energy characteristics of the Synchronous Reluctance motor.

- 10.** Ken Chen, Wenfei Yu and Chuanxin Wen et al [10], have took two different strategies for rotor structure optimization and conclude that rotor structure with 4 flux barriers and 2.5 mm barrier width gives better torque and low torque ripple.

3

INDUCTION MOTOR

3.1 HISTORY AND DEVELOPMENT

In 1831 Faraday published the electromagnetic law of induction and around 1860 Maxwell formulated the equations for electricity known as Maxwell's equations. This knowledge was essential for the invention of the induction motor. In 1885 Galileo Ferraris and one year afterwards (1886) Nikola Tesla presented two types of motors where the operating principle can be recognized in today IM's. A rotating magnetic field in the stator induces currents in rotor bars or windings that produces the torque of the motor.

This principle was taken to industrial use by Dolivo-Dobrovolsky whom also invented the wound and cage rotor around year 1889 and in 1900 the motor was ready for wide industrial use. One of the key benefits of the IM is the non-zero torque at zero speed which means that it is self-starting. This allows the motor to be grid connected without an external starting device. The IM has been known to be called "The work horse" of the industry since its introduction in the industry and with modern technology the IM have improved in all areas and has reached its peak in performance regarding efficiency and power density.

3.2 WORKING PRINCIPLE

A typical IM consists of a multiphase stator winding that produce a magnetic field that induces current in short circuited windings or in the rotor bars. The induced current produces the torque of the motor. In order for the motor to generate active torque there needs to be a speed difference between the rotating electric field in the stator and the speed of the rotor known as slip, s .

This slip is defined in equation and is causing ohmic losses in the rotor during steady state that is proportional to the slip times the output power of the motor.

$$S = \frac{\omega - \omega_r}{\omega}$$

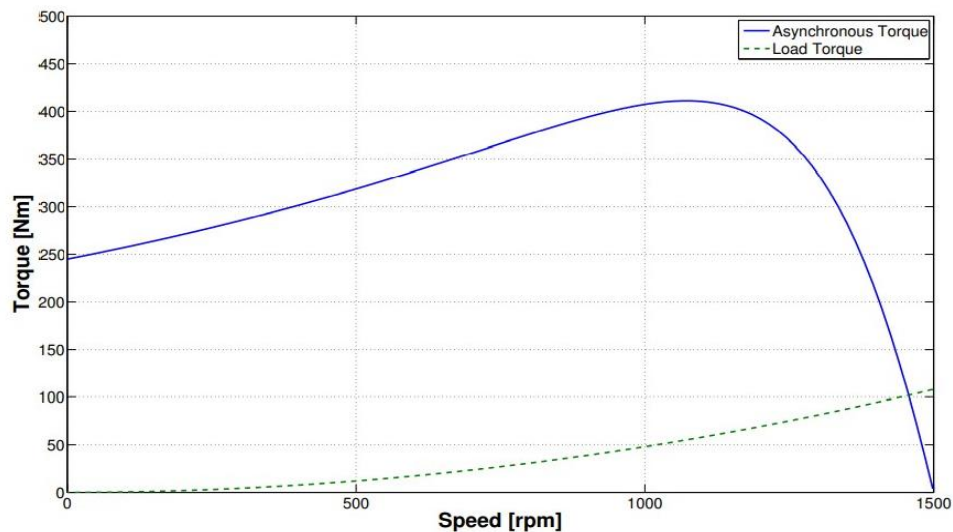


Figure 8: Torque speed curve for a typical IM with quadratic load torque.

In Figure 1.1 a typical IM torque characteristic can be seen together with a quadratic load characteristic. The motor will operate at the point of intersection which corresponds to a certain torque and speed.

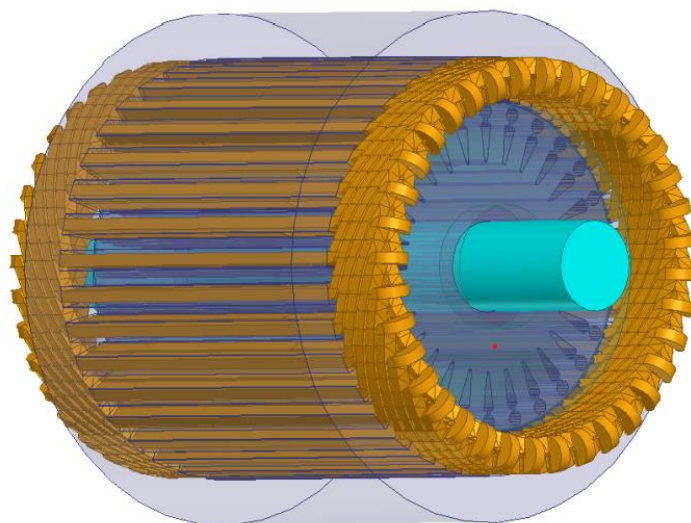


Figure 9: Squirrel cage induction motor.

The robustness, low cost and the ability of direct on-line starting have made the IM a common choice for constant speed applications but at lower power ratings especially between 5 kW - 30 kW the efficiency can be improved.

3.3 STATOR DESIGN

The stator is made of laminated iron with slots of different shapes filled with copper or aluminium windings. Commonly, it has 2-6 poles and is operated from a three phase AC source.

In this project the focus will not be on the stator design. Any comparison between motors in this project will be made with the same stator. The stator used in the simulations is constructed as similar as possible with an existing motor specification given in the name plate details.

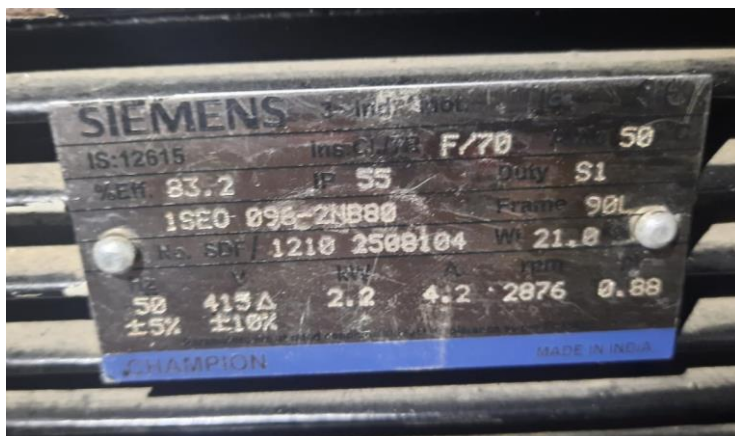


Figure 10: Name plate details of 90L framed induction machine

With the help of name plate details, we calculate and verify input power, synchronous speed, KVA rating, Armature current, stator slots, total number of conductors, efficiency, input current and slip using predefined formulae.

3.3.1 CALCULATION

- SPECS: rated power = 2.2kW, number of poles = 4, efficiency =83.21%
- KVA rating = output power/ (efficiency *power factor)
 $= (2.2) / (0.88*0.8321)$
 $= 3 \text{ KVA}$
- Synchronous speed, $N_s = (2*f) / p = (2*100) / 4 = 50 \text{ rps (or)}$

$$\begin{aligned} N_s &= (120*f) / p \\ &= (120*100) / 4 \\ &= 3000 \text{ rpm} \end{aligned}$$
- Slip of the machine = $(N_s-N_r) / N_s$ (rotor shaft speed =2876 rpm)

$$\begin{aligned} &= (3000-2876) / 3000 \\ &= 0.041 \end{aligned}$$
- Armature current = p / v

$$\begin{aligned} &= (2.2*10^3) / 440 \\ &= 5 \text{ A} \end{aligned}$$

We choose three slots per phase,

- Stator slots = (no of phases *poles *q)
 $= (3*4*3) = 36$
- Input power = $\sqrt{3}*v*i*\cos\theta$

$$\begin{aligned} &= \sqrt{3}*440*4.19*0.88 \\ &= 2.650 \text{ kW} \end{aligned}$$

We choose 80 conductors per slot,

- Total no of conductors, $Z = (\text{no of conductors per slot} * \text{total slots})$

$$Z = (80*36) = 2880 \text{ conductors}$$
- Efficiency = output power/input power

$$= p_o/p_i$$

- $P_i = \sqrt{3} * 440 * I * 0.88$
- $I = \text{input power} / 670.65$
 $= 2.65 * 10^3 / 670.65$
 $= 3.951 \text{ A}$

3.4 ROTOR DESIGN

The rotor can either be constituted by windings or bars, leaving two categories, wound rotor and squirrel cage rotor. The squirrel cage rotor is the most common because of its simple design and variety. The squirrel cage is enclosed in laminated iron which makes the rotor very robust. It consists of bars that are short circuited at the ends by so called end rings.

The bar shape and placement have a strong influence on the motor performance. It normally consists of aluminium but copper is also known to be used in high efficiency applications.

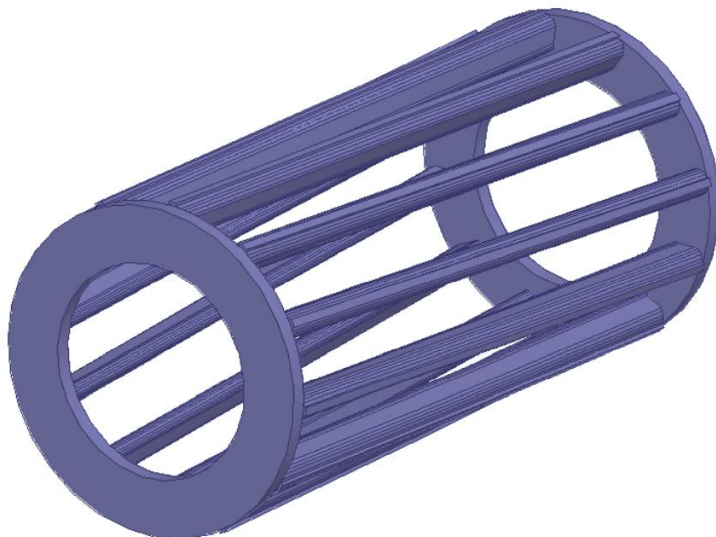
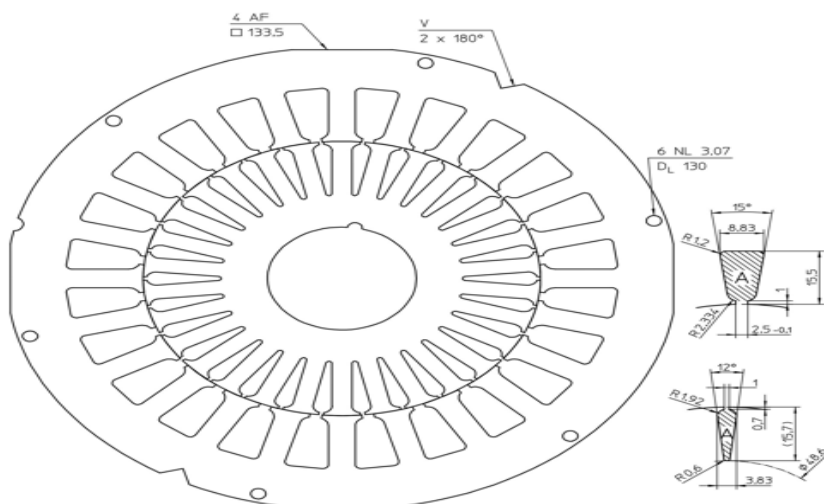


Figure 11: Typical squirrel cage with skew and end rings at both ends

3.5 GEOMETRY DATA

We figure out the geometry data for both stator and rotor from Kienle Spiess. Using this data, we find Stator Lam Dia, Tooth Width, Slot Depth, Slot Corner Radius, Tooth Tip Angle and Slot Opening for Stator. For Rotor, we find Bar opening, Bar opening Depth, Bar opening Radius, Rotor Tooth Width, Bar Depth, Bar corner Radius and shaft Dia.



| IEC 90/4.824 | | Maße und Varianten | | | | |
|----------------------|---------------|--------------------|----------------|----------|-------------|----------------|
| SB 135.08.X00 | | D _a | D _b | N | A | b _x |
| 04 | wie Abbildung | 135 +0.08 | 80x0.037 | 24 | 102.9 | 5.4 |
| | | | | AF, o NL | | |
| RB 080.02.Y.00 | | d _a | | N | A | b _x |
| 01 | 30 +0.033 M | 80 | | 30 | 38 | 4 |
| 04 | 20 +0.033 M | 05 | 25 +0.033 M | 03 | 22 +0.033 M | |
| Blechdicke SB und RB | | 0.5 | | | | |

These lamination drawings are meant for information only. PDF or DXF data will be provided upon request.
Dies ist eine unverbindliche Schnittzeichnung. PDF oder DXF Daten erhalten Sie auf Anfrage.

© 2003-2015 Kienle + Spiess GmbH

Figure 12: Geometry Data for Stator and Rotor

| Stator Dimensions | Value |
|--------------------|-------|
| Slot Number | 36 |
| Stator Lam Dia | 135 |
| Stator Bore | 80 |
| Tooth Width | 4 |
| Slot Depth | 15.5 |
| Slot corner Radius | 1.2 |
| Tooth Tip Depth | 0.66 |
| Slot Opening | 2.3 |
| Tooth Tip Angle | 10 |

Table 1: Stator Geometry Data

| Rotor Dimensions | Value |
|--------------------|-------|
| Rotor Bars | 26 |
| Pole Number | 4 |
| Bar Opening | 1 |
| Bar Opening Depth | 0.5 |
| Bar Opening Radius | 1.92 |
| Rotor Tooth Width | 4 |
| Bar Depth | 15.4 |
| Bar Corner Radius | 0.62 |
| Shaft Dia | 24 |

Table 2: Rotor Geometry Data

3.6 SIMULATION RESULTS

Using ANSYS MOTOR-CAD tool, we simulate the 90L framed IM model discussed in this chapter.

| Variable | Value | Units |
|-------------------------------|---------|-------|
| Shaft Torque | 7.6448 | Nm |
| Output Mechanical Power | 2305.6 | Watts |
| Input Active Electrical Power | 2770.1 | Watts |
| Input Reactive Power | 2415.6 | VA |
| Apparent Power | 3676.8 | VA |
| Power Factor | 0.75383 | |
| System Efficiency | 83.231 | % |

Table 1: Simulation output data

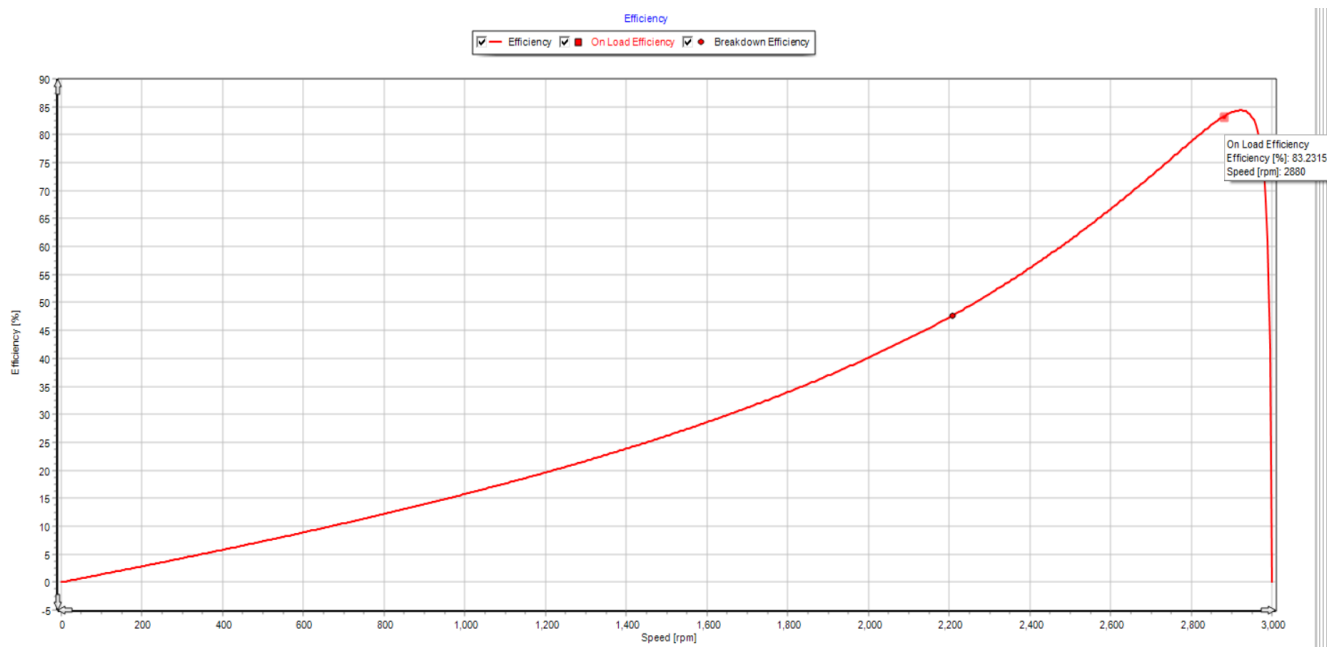


Figure 13: Efficiency vs Speed

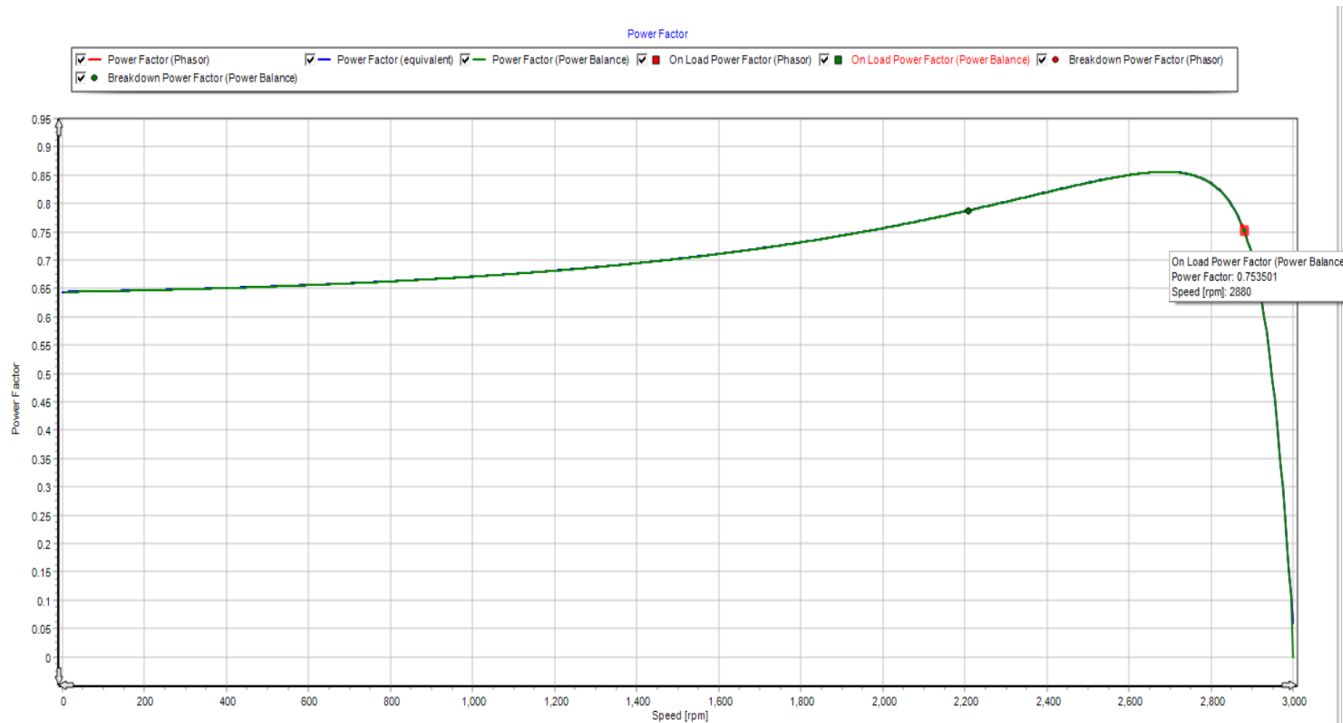


Figure 14: power factor vs Speed

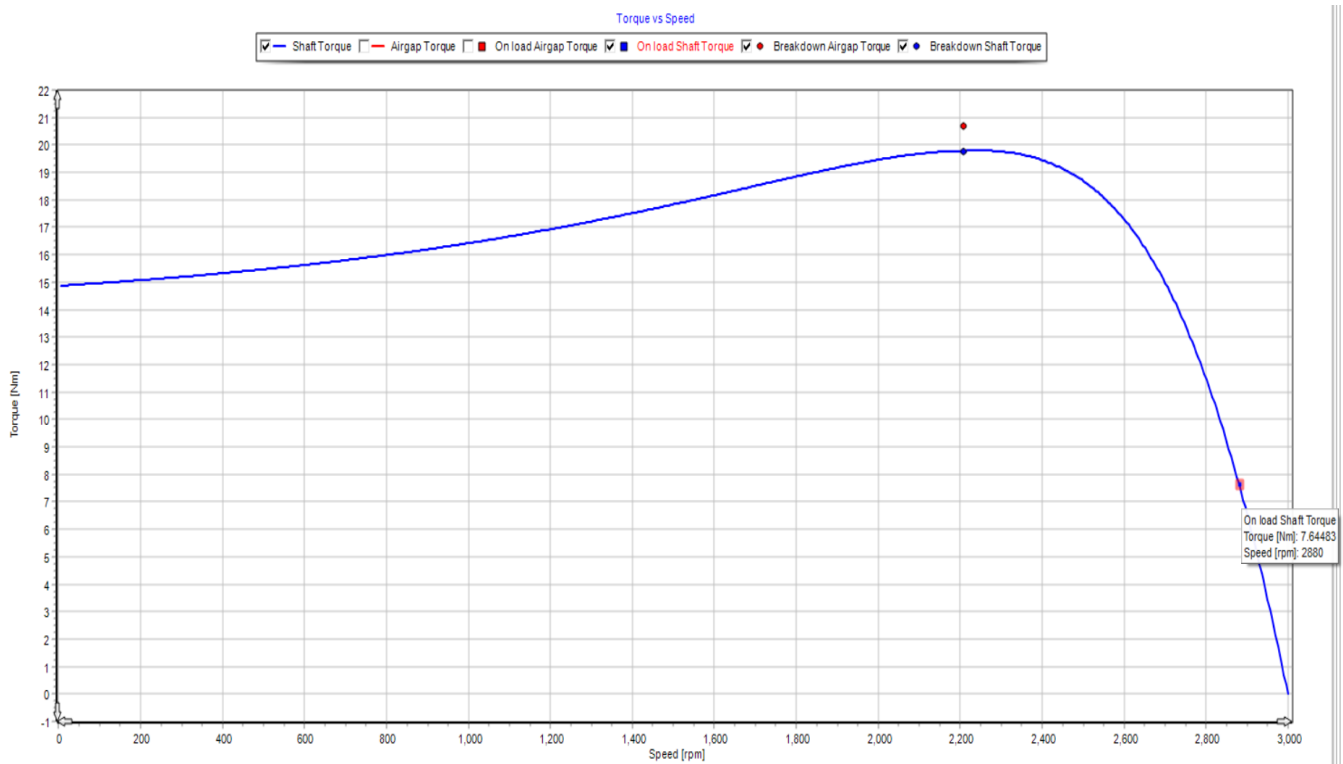


Figure 15: Torque vs Speed

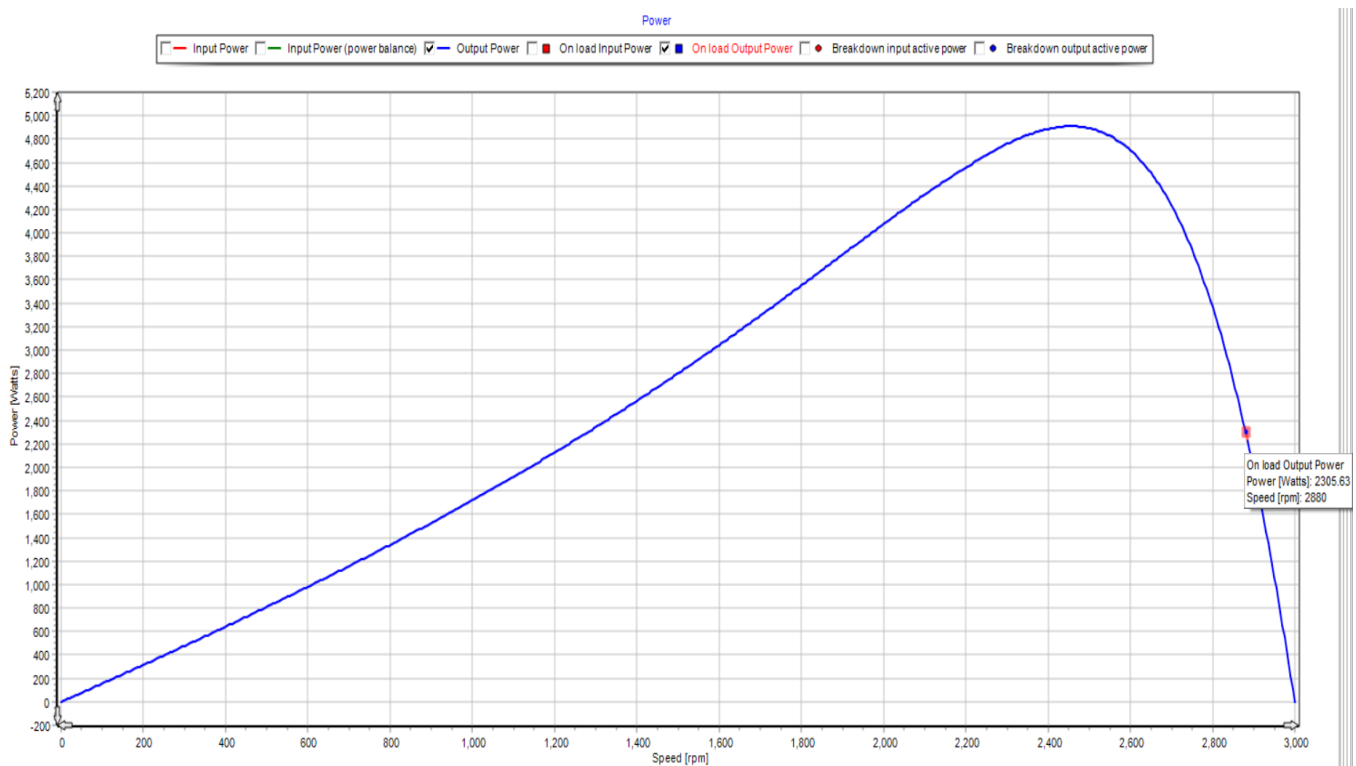


Figure 16: Power vs Speed

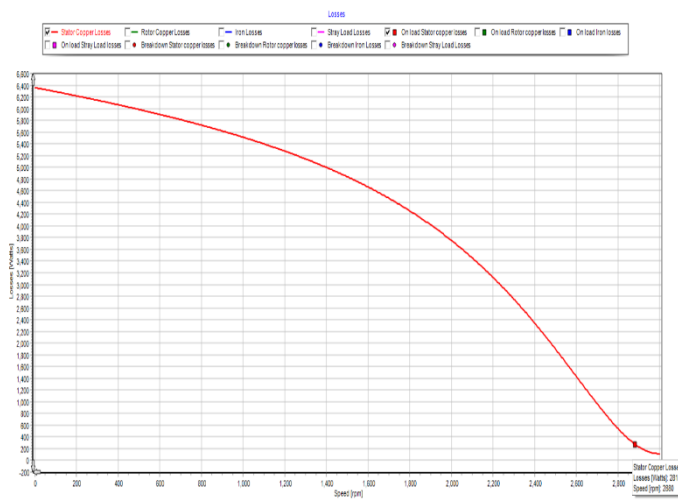


Figure 18: stator copper loss

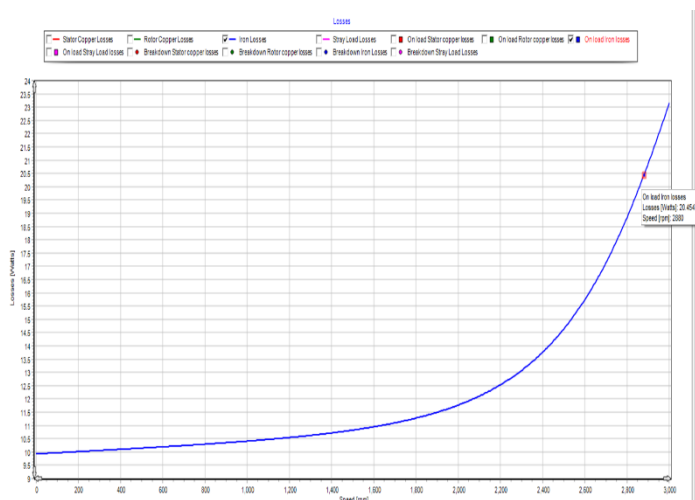


Figure 17: On load Iron loss

3.7 LOSS DISTRIBUTION

With new tougher environmental guide line the industry is pushed to more and more efficient motors. The highest class, IE4, is difficult for a middle size IM to reach.

In order to find a advanced motor that can compete with the IM it is important to identify and localize the losses in the induction motor. They can be divided as follows:

- Stator copper losses, PCu1
- Rotor copper losses, PCu2
- Core iron losses, Pfe1
- Friction and windage losses, Pmech
- Stray losses, Pstray

The stator copper losses are the biggest source of losses in the motor. Next is the rotor copper losses and the core losses. The stray losses are due to eddy currents in the motor and are hard to localize. They vary from one design to another and are located both in the stator and rotor.

For a typical IM around 20 kW of output power the losses are distributed as depicted in figure 1.13. Other losses consist of core iron losses, friction losses, windage losses and stray losses.

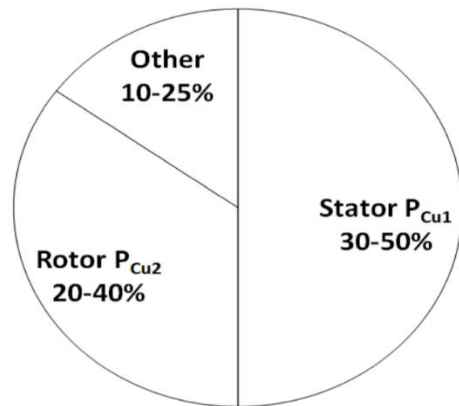


Figure 19: Typical loss distribution for an induction motor

Since the stator for a IM and a SynRM are very similar it is in the rotor the biggest reduction of the losses can be made.

4

SYNCHRONOUS RELUCTANCE MACHINE

4.1 INTRODUCTION

Synchronous reluctance machine with traversally laminated rotor design was proposed several years ago but only in the past few years it is becoming more and more attractive among engineers and companies. This can be said due to its robustness and high overload capability. It is also low cost design product. The REL motor is becoming good competitor in applications requiring high dynamics and high torque production capability along with fault tolerant capability.



Figure 20: SynRM Rotor

4.2 SYNCHRONOUS RELUCTANCE MOTOR

There are two different paths for flux flow. one is the high permeability path for the flow of the flux lines along the rotor iron path. parallel to the flux barriers. It is generally referred to as the d-axis path. the second one is the low permeability path since the flux lines have to cross the flux barriers that area present in the rotor. This path is referred to as q axis path.

The rotor is designed with several flux barriers in order to obstacle along the q axis and to achieve a higher saliency ratio that is high reluctance torque component.

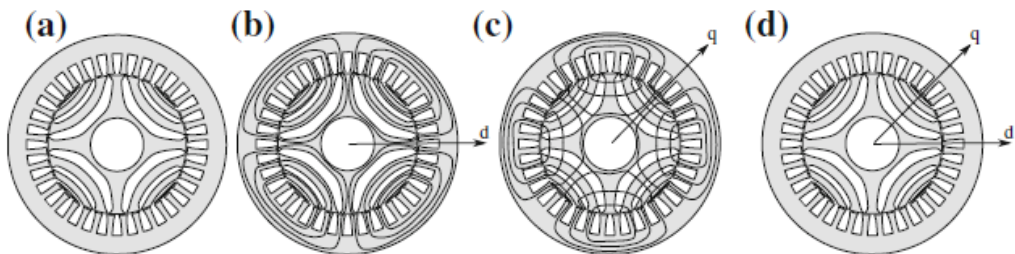


Figure 21: Sketch of a synchronous reluctance motor with

- a- Geometry
- b- D axis flux
- c- Q axis flux
- d- Reference frame (d and q axis flux lines)

4.3 WORKING

The alternating current that which passes through the stator windings creates a rotating magnetic field in the air gap of the Synchronous reluctance motor. Torque will be created when the SynRM tries to establish its most magnetically conductive axis (direct axis) (d-axis) with an applied field in order to minimize the reluctance (magnetic resistance) in the magnetic circuit. The magnitude of the torque obtained Is the directly proportional to the difference in the direct L_d and quadrature L_q inductances.

Therefore, the greater the difference, the greater the torque created. Thereby lower will be the torque ripple.

In a synchronous reluctance motor, the magnetic field will be created by a sinusoidally distributed stator winding. The field rotates at synchronous speed and will be considered sinusoidal.

In such a situation, there will always be a torque aimed at reducing the whole system potential energy by reducing the field distortion along the q axis. If the angle δ is kept constant, for example, by controlling the magnetic field, then the electromagnetic energy will be continuously converted into mechanical energy.

The stator current is the responsible for magnetization and it is also responsible for creating a torque that attempts to reduce field distortion. The torque along with power factor is controlled by controlling the current angle (k), that is, the angle between the current vector of the stator winding and the rotor d-axis in a rotating coordinate system.

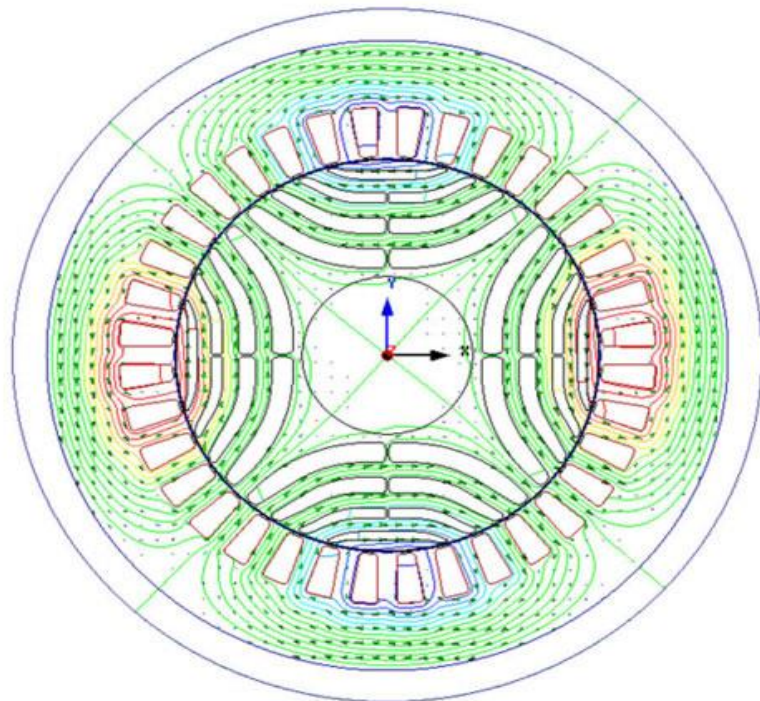


Figure 22: Cross sectional view of SynRM motor.

4.4 PERFORMANCE

The Synchronous reluctance motor (SynRM) has become commercially viable as a high efficiency alternative to the induction motor in recent years. The core idea of a SynRM motor is that the rotor has no windings or magnets, just electric steel plates stacked together to form a rotor package.

Unlike in an induction motor, a SynRM rotor has no induced current and thus no losses. This makes SynRM the perfect combination of simplicity and efficiency. The synRm has better torque production capabilities. even with low power factor the efficiency is relatively high.

Torque ripple also can be reduced in SynRM.

5

IMPLEMENTATION OF 3 FLUX BARRIER MODEL

5.1 INTRODUCTION

In order to reduce the torque ripple percentage and to produce better power factor the no of flux barriers in the SynRM rotor needs to be increased. The higher the no of flux barriers the higher will be the saliency ratio and better will be the power factor of the machine

5.2 SYNRM GEOMETRY FOR 3 FLUX BARRIERS

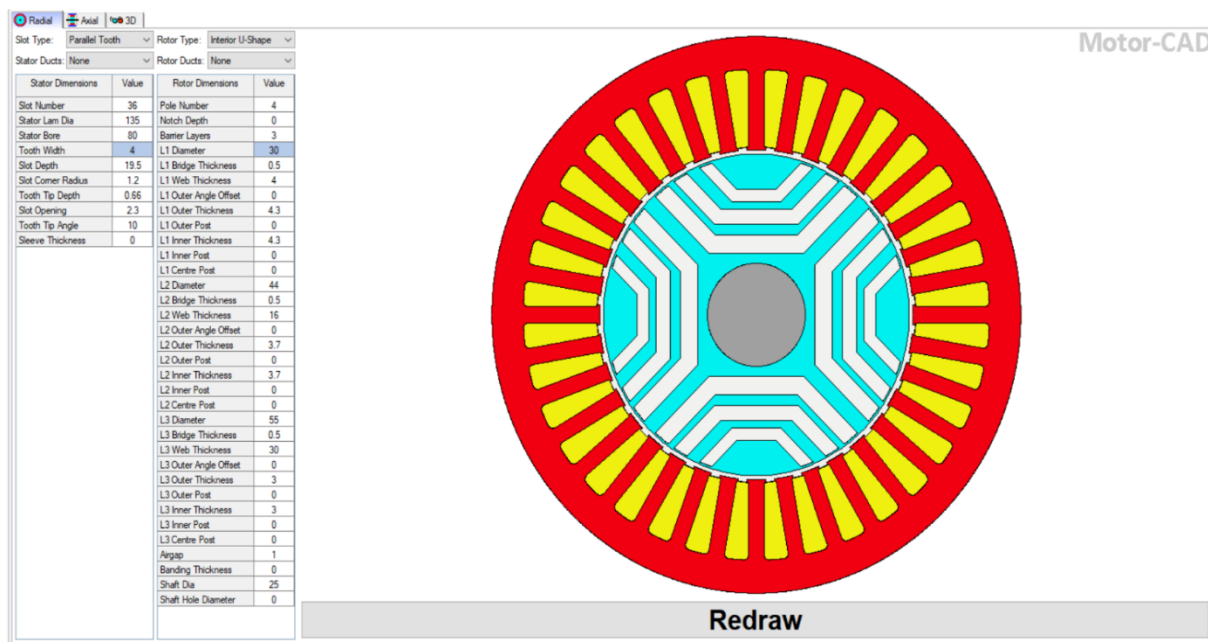


Figure 23: SynRM Stator and Rotor Geometry

5.3 DESIGN PARAMETERS

The stator part of the synchronous reluctance machine is the same as that of the induction machine. only the rotor structure is redesigned. An interior U-Shape rotor structure is chosen for our design. The project goal is to model a SynRM with rating 2.2kw, 4 pole machine with 3000rpm rated speed. The 3 barriers are chosen such that with each barrier the barrier thickness tends to increase in order to oppose flux flow in q axis side thereby reducing q axis inductance.

The no of stator slots has been chosen to be 36 such that there will be 3 slots per phase.

$$\text{Stator slots} = (\text{no of phases} * \text{poles} * q)$$

As $q=3$,

$$\text{Stator slots} = (3 * 4 * 3)$$

$$= 36 \text{ slots}$$

- No of poles: 4
- Slot depth – 19.5mm
- Tooth width- 4mm
- Stator lamination diameter -135mm
- L1 Diameter -30mm
- L2 Diameter -44mm
- L3 Diameter -55mm
- Airgap thickness -1mm
- Stack length – 95mm

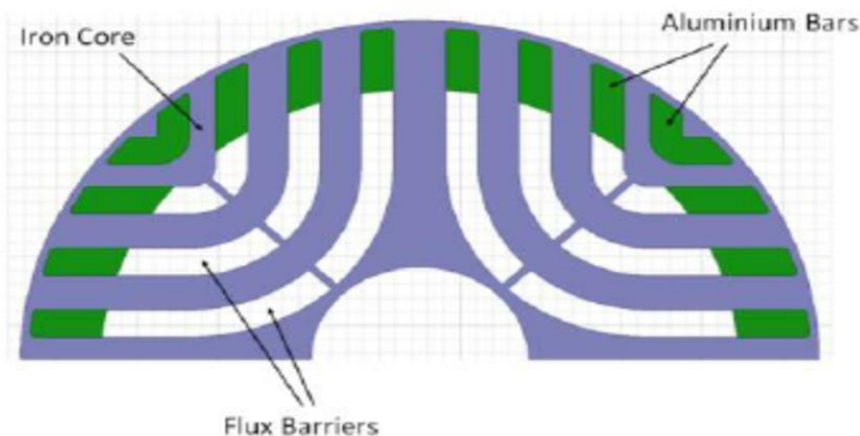


Figure 24: SynRM Model with 3 flux barriers

5.4 SYNRM GEOMETRY - AXIAL VIEW

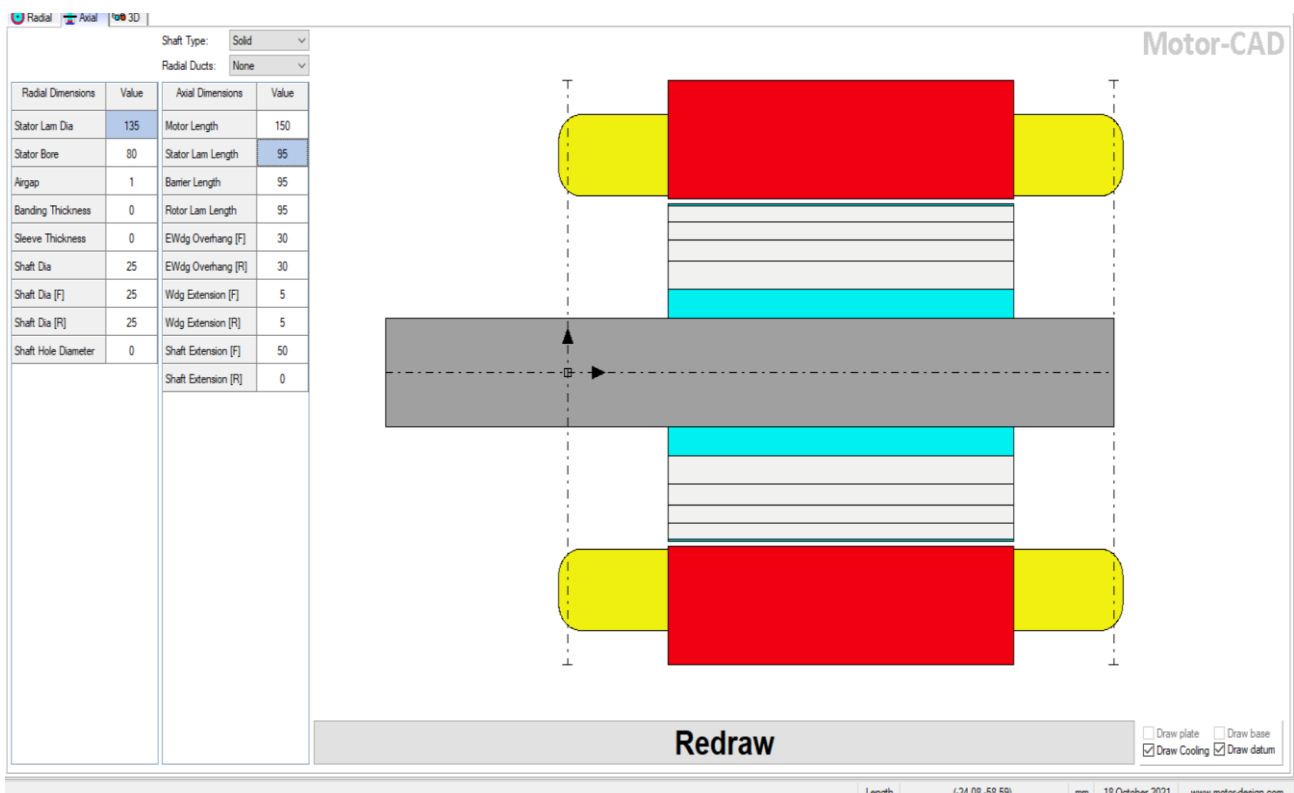


Figure 25: Axial View

5.5 WINDING

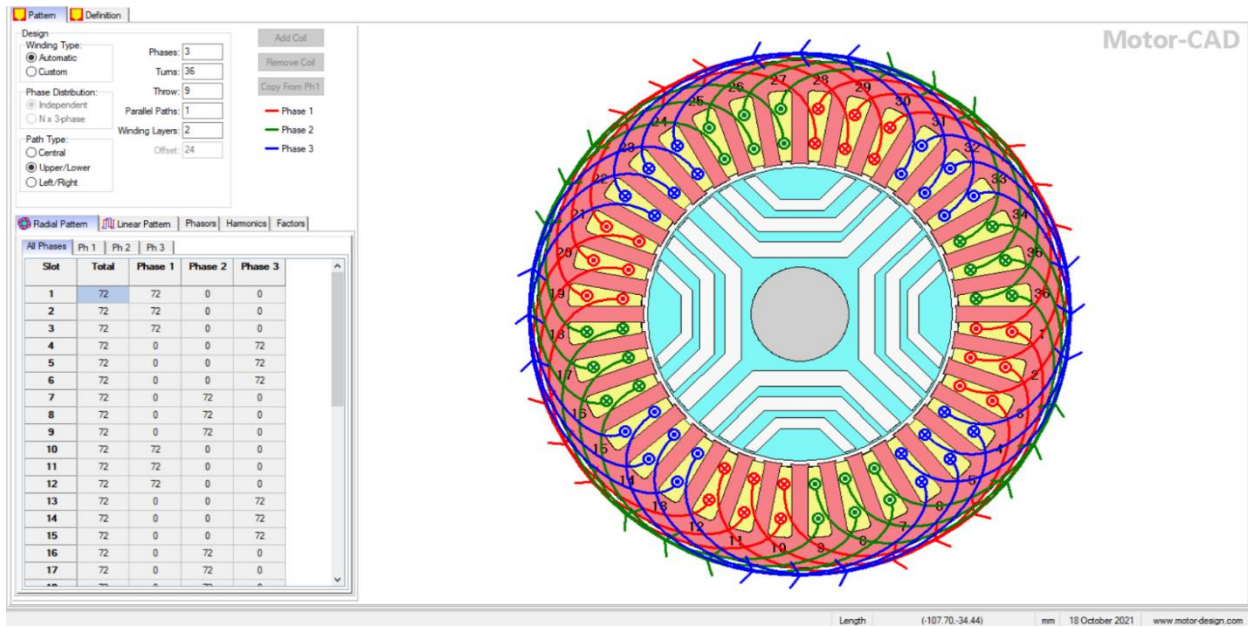


Figure 26: Winding pattern

1. Winding type - 3 phase star connected winding

2. Coil pitch (throw value) = (no of slots)/poles

$$= 36/4$$

$$= 9 \text{ (same as in induction machine)}$$

3. Number of Coils = (36/2)

$$= 18$$

4. Number of coils per phase = (18/3)

$$= 6 \text{ coils per phase.}$$

5.6 3D MODEL OF SYNRM

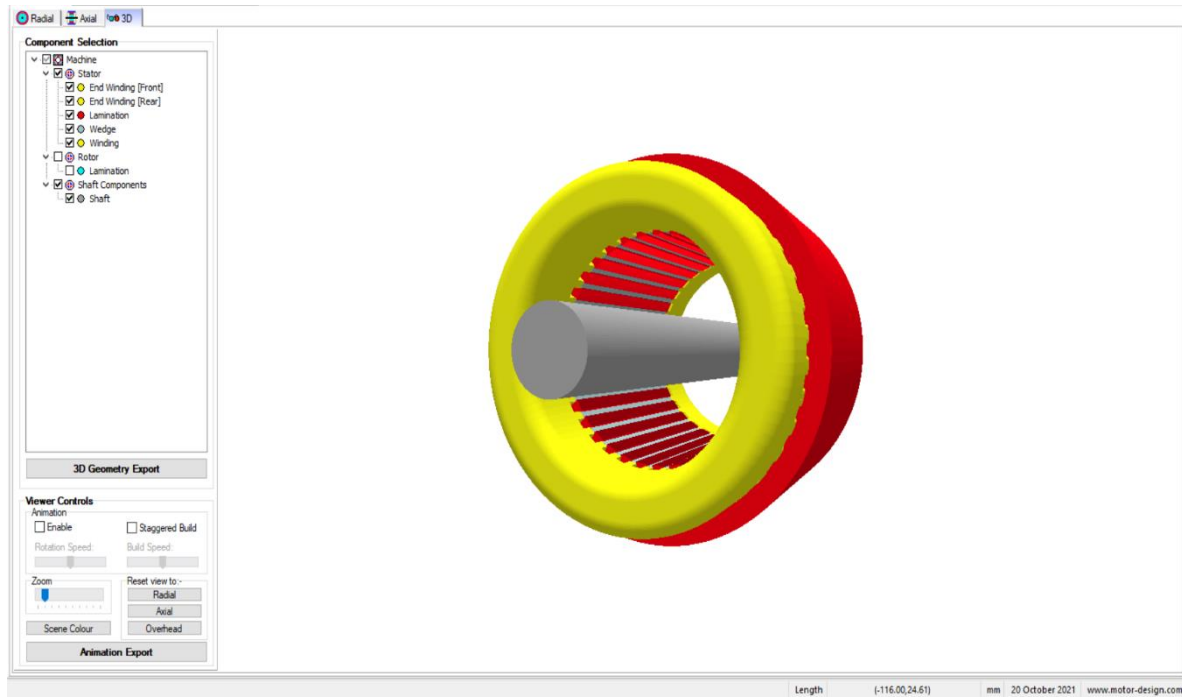


Figure 27: 3D Model of SynRM

5.7 MATERIALS USED FOR STATOR AND ROTOR DESIGN

M19 29 Gauge steel is chosen for both stator and rotor lamination.

M19 are available in three thickness (0.0140 inch, 0.0185 inch and 0.0250 inch) with core loss of 1.55W/lb, 1.65W/lb and 2.0 W/lb respectively. M19 29 gauge or M19 26 gauge can be chosen for this model. The main difference applies in core losses, thickness and application. As 26gauge steel has high core losses we move with M19 29 Gauge steel for this application.

| Component | Material from Database |
|------------------------------|------------------------|
| Units | |
| Stator Lam (Back Iron) | M19 29 Gauge Steel |
| Stator Lam (Tooth) | M19 29 Gauge Steel |
| Stator Lamination [Total] | |
| Amature Winding [Active] | Copper (Pure) |
| Amature EWdg [Front] | Copper (Pure) |
| Amature EWdg [Rear] | Copper (Pure) |
| Amature Winding [Total] | |
| Slot Wedge | |
| Rotor Lam (Back Iron) | M19 29 Gauge Steel |
| Rotor Lam (IPM Magnet Pole) | M19 29 Gauge Steel |
| Rotor Lam (Inter Magnet Gap) | M19 29 Gauge Steel |
| Rotor Lamination [Total] | |
| Shaft [Active] | Copper (Pure) |
| Shaft [Front] | Copper (Pure) |
| Shaft [Rear] | Copper (Pure) |
| Shaft [Total] | |
| Total | |

Figure 28: Materials Chosen for Stator and Rotor

5.8 INPUT PARAMETERS

These details are obtained from the name plate of SynRM.

The shaft speed of the motor is 3000 rpm. As it is a synchronous machine the stator mmf speed and rotor rotation speed is the same. The peak current of the motor is 5.5A. DC bus voltage was set as 535 V.

| | |
|---|---|
| Drive: | Shaft Speed: <input type="text" value="500"/> |
| Line Current Definition: | |
| <input checked="" type="radio"/> Peak <input type="radio"/> RMS <input type="radio"/> RMS Current Density | |
| Peak Current: | <input type="text" value="5.5"/> |
| RMS Current: | <input type="text" value="3.889"/> |
| RMS Current Density: | <input type="text" value="7.902"/> |
| DC Bus Voltage: | <input type="text" value="535"/> |
| Phase Advance [elec deg]: | <input type="text" value="67"/> |
| Drive: | |
| Drive Type: <input checked="" type="radio"/> Defined Currents (Default) <input type="radio"/> Calculated Currents | |
| Drive Mode: <input checked="" type="radio"/> Sine <input type="radio"/> Square <input type="radio"/> Custom <input type="radio"/> Passive Generator | |
| Winding Connection: | |
| <input checked="" type="radio"/> Star Connection (default) <input type="radio"/> Delta Connection | |
| Magnetisation: | |
| <input checked="" type="radio"/> Parallel <input type="radio"/> Radial <input type="radio"/> Halbach Continuous Ring Array <input type="radio"/> Halbach Sinusoidal Array | |
| Temperatures: | |
| Armature Winding Temperature: <input type="text" value="40"/> Magnet Temperature: <input type="text" value="20"/> Stator Lamination Temperature: <input type="text" value="20"/> Rotor Lamination Temperature: <input type="text" value="20"/> Stator Sleeve Temperature: <input type="text" value="20"/> Rotor Banding Temperature: <input type="text" value="20"/> Shaft Temperature: <input type="text" value="20"/> Armature Wedge Temperature: <input type="text" value="20"/> Housing Temperature: <input type="text" value="20"/> | |
| E-Magnetic ↔ Thermal Coupling: | |
| E-Magnetic ↔ Thermal Coupling: <input checked="" type="radio"/> No coupling (default) <input type="radio"/> E-Magnetic Losses → Thermal <input type="radio"/> E-Magnetic ← Thermal Temperatures <input type="radio"/> Iterate to Converged Solution | |
| Skew: | |
| Skew Type: <input checked="" type="radio"/> None (default) <input type="radio"/> Stator <input type="radio"/> Rotor | |
| Stator Skew: <input type="text" value="0"/> Rotor slices: <input type="text" value="1"/> | |
| Performance Tests: | |
| Single operating points: <input type="checkbox"/> Open Circuit <input type="checkbox"/> Q axis current only <input checked="" type="checkbox"/> On Load | |
| Open Circuit: | |
| <input type="checkbox"/> Back EMF <input type="checkbox"/> Cogging Torque <input type="checkbox"/> Electromagnetic Forces | |
| On Load: | |
| <input checked="" type="checkbox"/> Torque <input checked="" type="checkbox"/> Torque Speed Curve <input type="checkbox"/> Demagnetization <input type="checkbox"/> Electromagnetic Forces | |
| Parameters: | |
| <input type="checkbox"/> Self and Mutual Inductances | |
| Transient: | |
| <input type="checkbox"/> Sudden short-circuit | |
| Solve E-Magnetic Model | |
| Cancel Solving | |

Figure 30: Input Details



Figure 29: Name plate details

5.9 OUTPUT

| Variable | Value | Units |
|---|-------------|--------------------|
| Maximum torque possible (DQ) (For Phase Advance of 50 EDeg) | 8.9911 | Nm |
| Average torque (virtual work) | 7.2999 | Nm |
| Average torque (loop torque) | 7.2342 | Nm |
| Torque Ripple (MsVw) | 2.9919 | Nm |
| Torque Ripple (MsVw) [%] | 41.002 | % |
| Speed limit for constant torque (For Phase Advance of 67 EDeg) | 1789.9 | rpm |
| No load speed | INF | rpm |
| Speed limit for zero current | 3468.2 | rpm |
| ----- | | |
| Electromagnetic Power | 2292.4 | Watts |
| Operating point outside voltage limit. | | |
| Input Power | 2630.2 | Watts |
| Output Power | 2275.8 | Watts |
| Operating point outside voltage limit. | | |
| Total Losses (on load) | 354.37 | Watts |
| System Efficiency | 86.527 | % |
| ----- | | |
| Shaft Torque | 7.2442 | Nm |
| ----- | | |
| Power Factor [Waveform] (lagging) | 0.63721 | |
| Power Factor Angle [Waveform] | 50.416 | EDeg |
| Power Factor [Phasor] (lagging) | 0.64279 | |
| Power Factor Angle [Phasor] | 50 | EDeg |
| Load Angle [Phasor] | 117.4 | EDeg |
| Phase Terminal Voltage (rms) [Phasor] | 353.28 | Volts |
| ----- | | |
| Rotor Inertia | 0.001329 | kg.m ² |
| Shaft Inertia | 6.8515E-005 | kg.m ² |
| Total Inertia | 0.0013975 | kg.m ² |
| Torque per rotor volume | 16.075 | kNm/m ³ |
| ----- | | |
| Motor B=0.177T μ R=8000 J=0A/mm ² C=0AT Area= 551.6mm ² | | |

Figure 31: Output Data Obtained for 3 Flux Barrier Model

5.10 GRAPHS

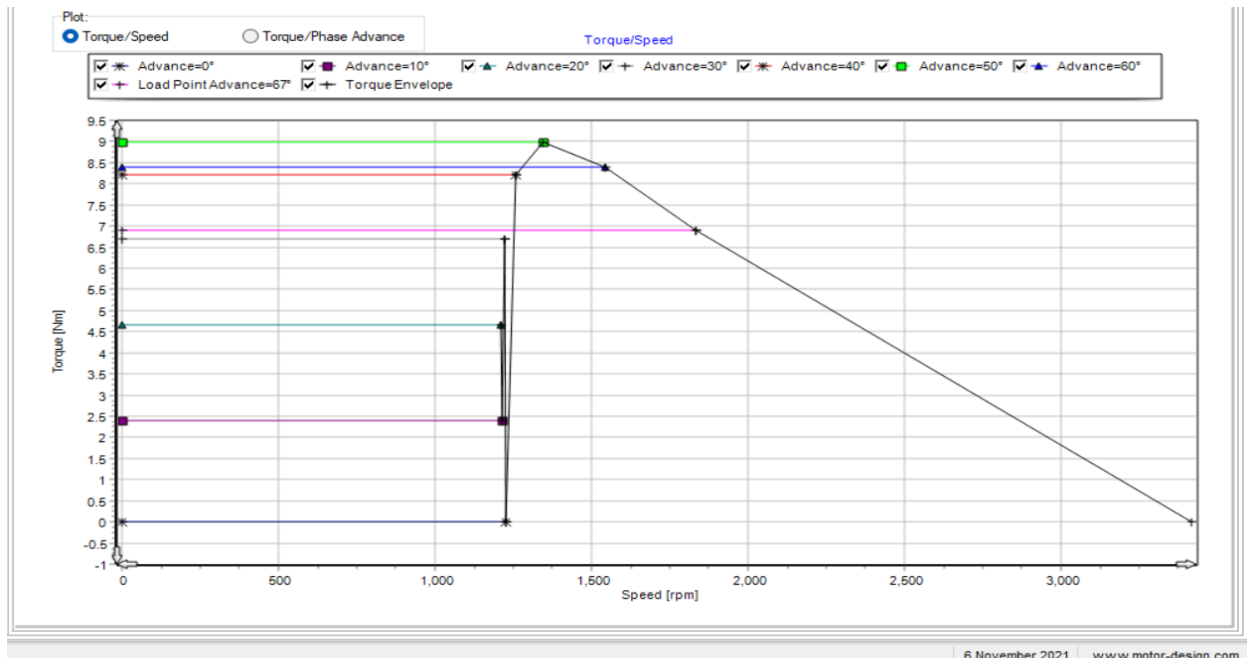


Figure 32: Torque vs Speed

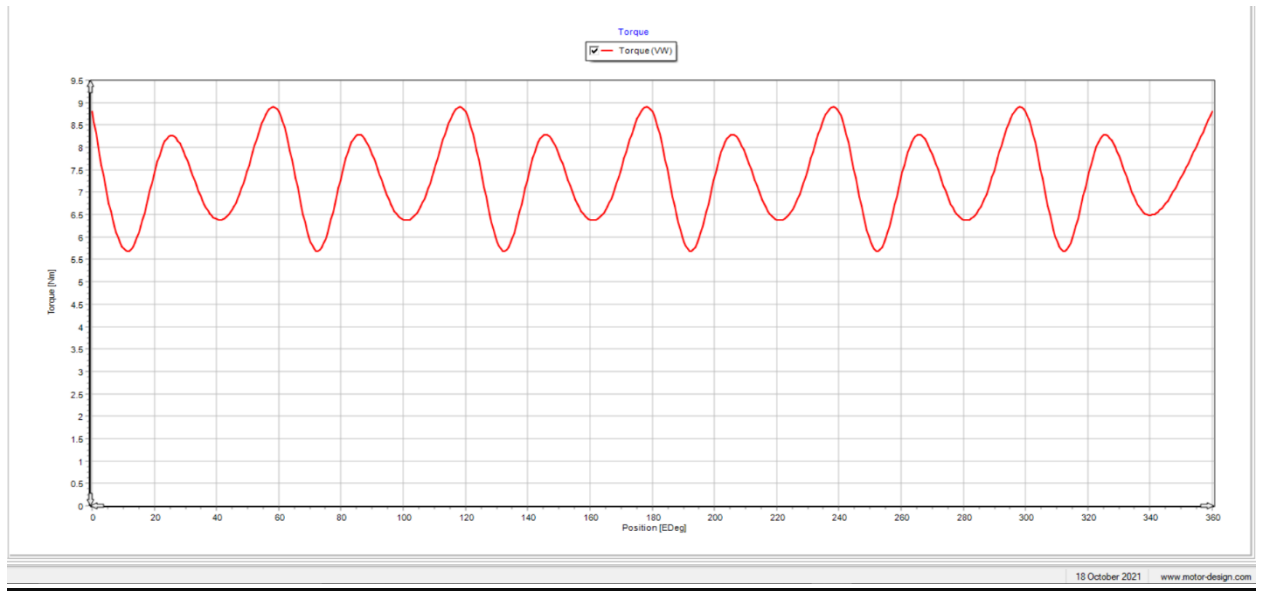


Figure 33: Torque vs Position

5.11 TORQUE RIPPLE

$$\begin{aligned}1. \text{ Average torque} &= (\text{max peak torque} + \text{min peak torque})/2 \\&= (8.8+5.8)/2 \\&= 7.3 \text{Nm (from graph)}\end{aligned}$$

Average torque as shown in simulation output is 7.2342 Nm

$$\begin{aligned}2. \text{ Torque Ripple} &= (\text{max peak torque} - \text{min peak torque}) \\&= 8.8-5.8 \\&= 3.0 \text{Nm}\end{aligned}$$

Torque ripple as shown in simulation output is 2.99 Nm

Theoretically calculated value:

% Torque ripple = $(\text{max peak torque} - \text{min peak torque})/\text{average torque}$

$$\begin{aligned}&= (8.8-5.8)/7.3 \\&= 41.09\end{aligned}$$

Software output:

%Torque ripple = (max peak torque – min peak torque)/average torque

$$= (3)/7.2342$$

$$= 41.46$$

5.12 E-MAGNETICS

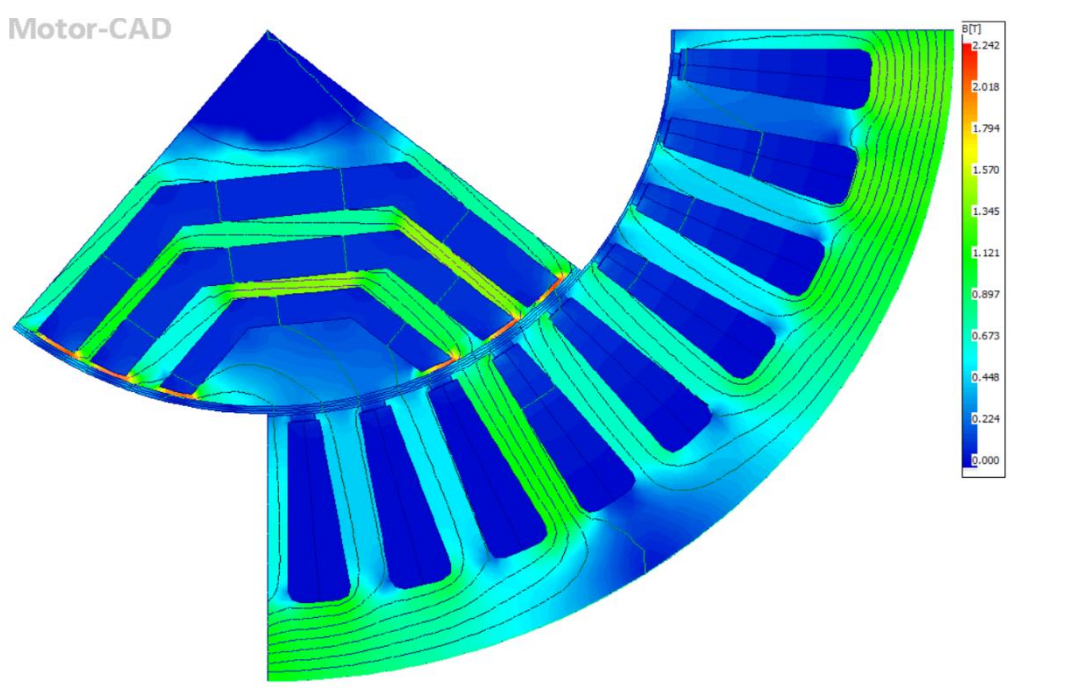


Figure 34:E-Magnetics for 3 Flux Barrier Model

6

MODELLING AND IMPLEMENTATION OF 4 FLUX BARRIER SYNRM

6.1 INTRODUCTION

The main reason for moving to 4 flux barrier model is that in 3 flux barrier model the % torque ripple is quite high in order to reduce the torque ripple we increase the no of flux barriers.

6.2 SYNRM MODEL WITH 4 FLUX BARRIERS

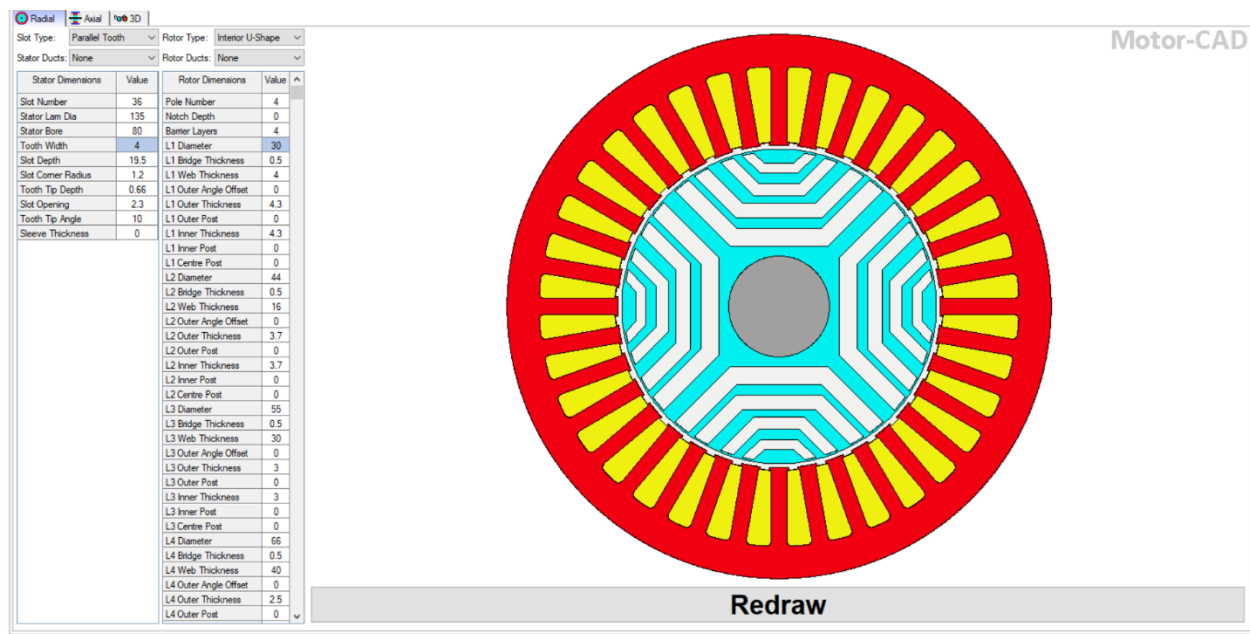


Figure 35: SynRM 4 Flux Barrier Model

6.3 AXIAL VIEW OF SYNRM

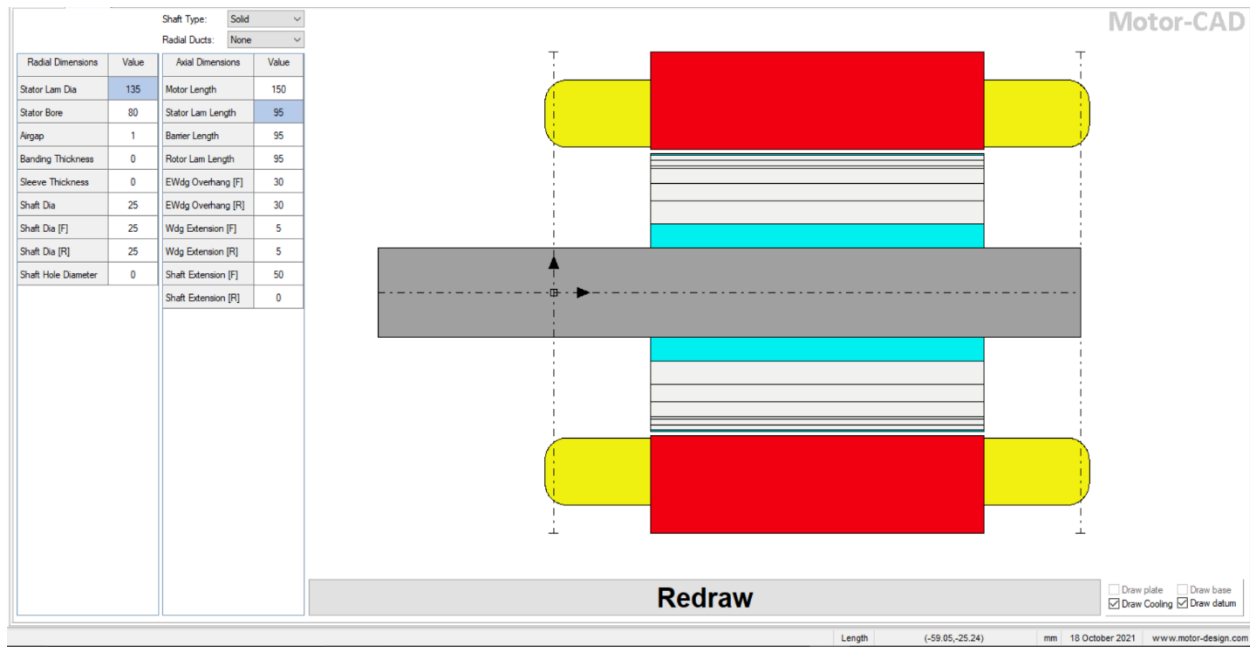


Figure 36: Axial view 4 Layer Barrier Model

6.4 3-D MODEL OF SYNRM

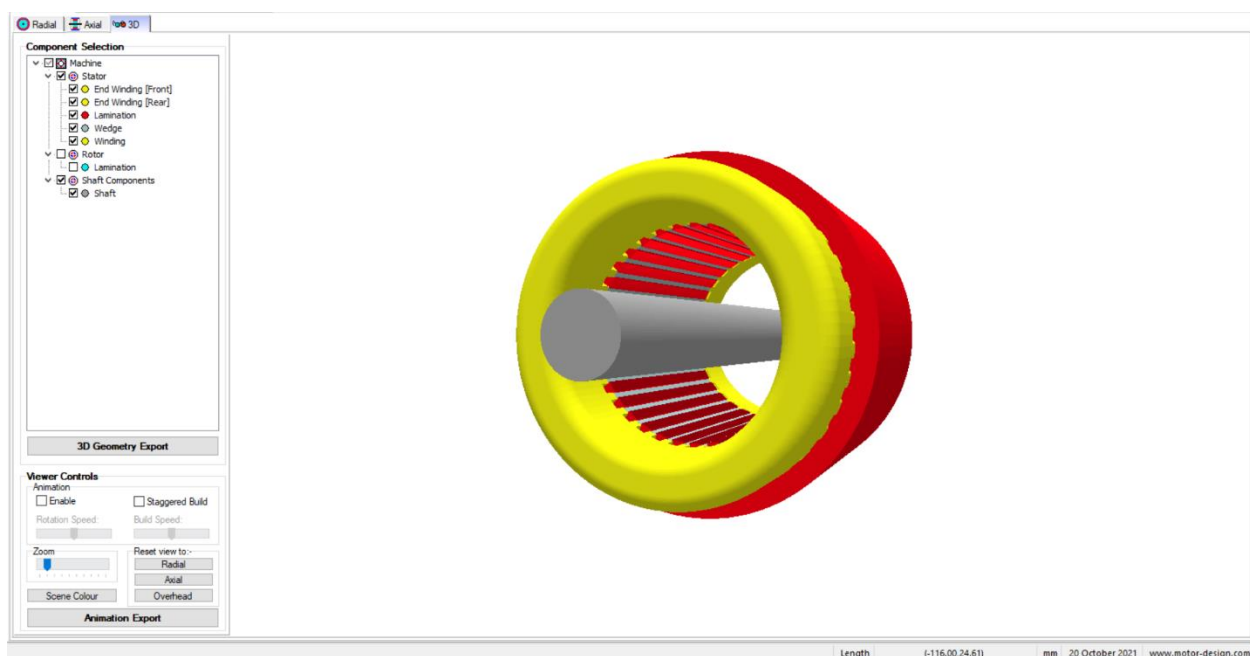


Figure 37: 3D model of 4 Layer Barrier Model

6.5 WINDING

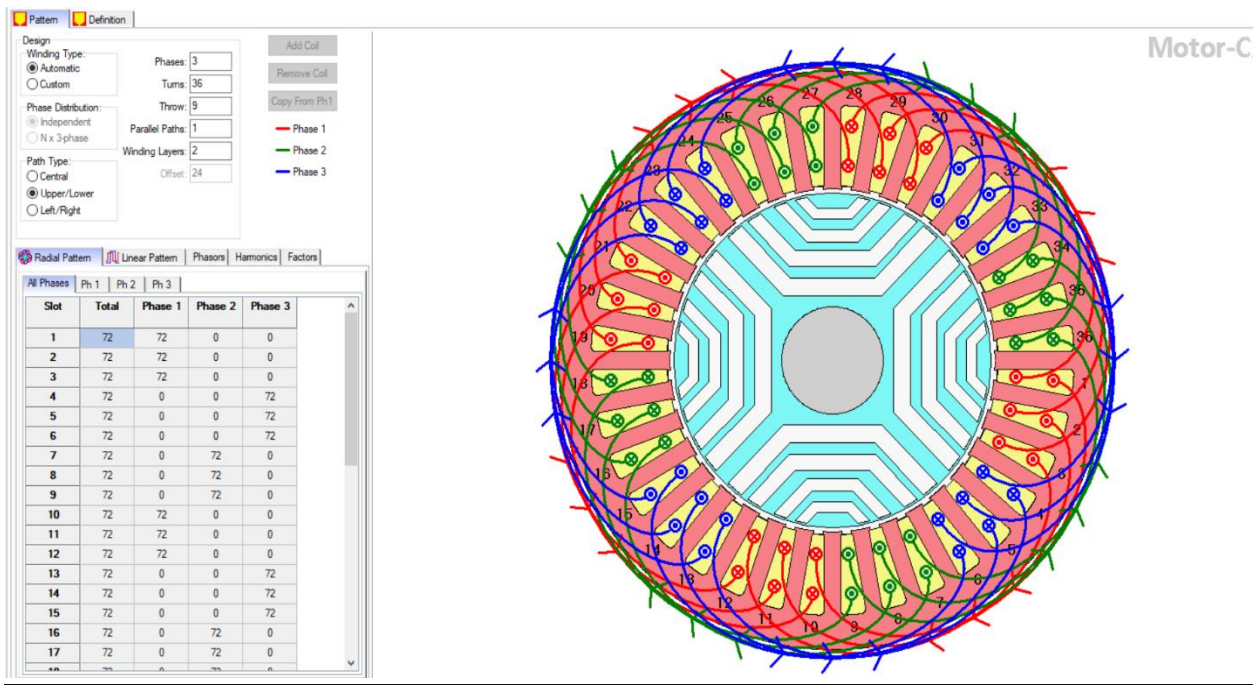


Figure 38: Winding Pattern

1. Winding type - 3 phase star connected winding
2. Coil pitch (throw value) = (no of slots)/poles
= $36/4$
= 9 (same as in induction machine)
3. Number of Coils = $(36/2) = 18$
4. Number of coils per phase = $(18/3) = 6$ coils per phase.

6.6 INPUT PARAMETERS

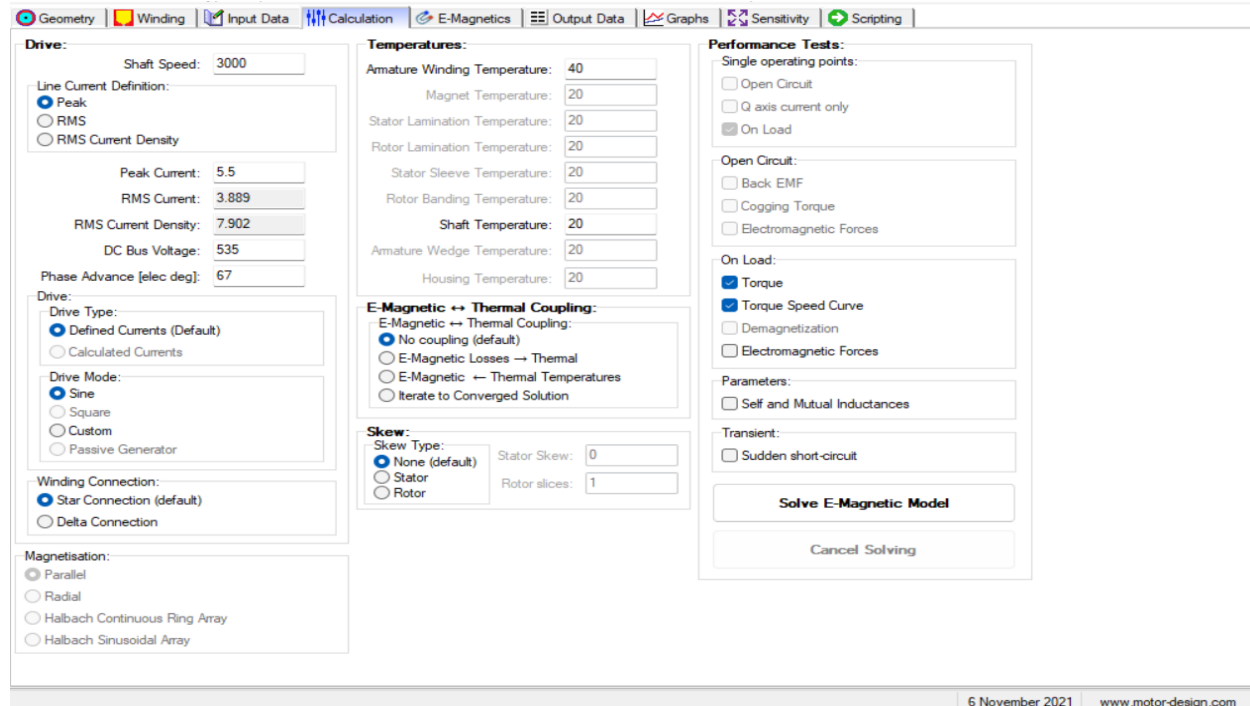


Figure 39: Input Details

Input details are same as that given in 3 layer flux barrier model as only geometry of the rotor design alone is changed for this 4 layer flux barrier model.

6.7 MATERIALS USED

| Component | Material from Database |
|------------------------------|------------------------|
| <u>Units</u> | |
| Stator Lam (Back Iron) | M19 29 Gauge Steel |
| Stator Lam (Tooth) | M19 29 Gauge Steel |
| Stator Lamination [Total] | |
| Armature Winding [Active] | Copper (Pure) |
| Armature EWdg [Front] | Copper (Pure) |
| Armature EWdg [Rear] | Copper (Pure) |
| Armature Winding [Total] | |
| Slot Wedge | |
| Rotor Lam (Back Iron) | M19 29 Gauge Steel |
| Rotor Lam (IPM Magnet Pole) | M19 29 Gauge Steel |
| Rotor Lam (Inter Magnet Gap) | M19 29 Gauge Steel |
| Rotor Lamination [Total] | |
| Shaft [Active] | Copper (Pure) |
| Shaft [Front] | Copper (Pure) |
| Shaft [Rear] | Copper (Pure) |
| Shaft [Total] | |
| Total | |

Figure 40: Materials used for Stator and Rotor

6.8 OUTPUT

| Variable | Value | Units |
|---|-------------|--------------------|
| Maximum torque possible (DQ) (For Phase Advance of 50 EDeg) | 9.1812 | Nm |
| Average torque (virtual work) | 7.4052 | Nm |
| Average torque (loop torque) | 7.3333 | Nm |
| Torque Ripple (MsVw) | 2.6204 | Nm |
| Torque Ripple (MsVw) [%] | 35.401 | % |
| Speed limit for constant torque (For Phase Advance of 67 EDeg) | 1804.6 | rpm |
| No load speed | INF | rpm |
| Speed limit for zero current | 3606.9 | rpm |
| ----- | | |
| Electromagnetic Power Operating point outside voltage limit. | 2325.4 | Watts |
| Input Power | 2663.2 | Watts |
| Output Power Operating point outside voltage limit. | 2309.7 | Watts |
| Total Losses (on load) | 353.54 | Watts |
| System Efficiency | 86.725 | % |
| ----- | | |
| Shaft Torque | 7.352 | Nm |
| ----- | | |
| Power Factor [Waveform] (lagging) | 0.65026 | |
| Power Factor Angle [Waveform] | 49.439 | EDeg |
| Power Factor [Phasor] (lagging) | 0.65606 | |
| Power Factor Angle [Phasor] | 49 | EDeg |
| Load Angle [Phasor] | 116.43 | EDeg |
| Phase Terminal Voltage (rms) [Phasor] | 350.33 | Volts |
| ----- | | |
| Rotor Inertia | 0.0012193 | kg.m ² |
| Shaft Inertia | 6.8515E-005 | kg.m ² |
| Total Inertia | 0.0012878 | kg.m ² |
| Torque per rotor volume | 16.306 | kNm/m ³ |

Stator B=1.252T μ R=4000 J= 0A/mm² C= 0AT Area= 1513mm²

Figure 41: Output Data for 4 Layer Flux Barrier Model

6.8.1 TORQUE RIPPLE

$$\begin{aligned}
 1. \text{ Average torque} &= (\text{max peak torque} + \text{min peak torque})/2 \\
 &= (8.7+6.0)/2 \\
 &= 7.35 \text{Nm (from graph)}
 \end{aligned}$$

Average torque as shown in simulation output is 7.4052 Nm

$$\begin{aligned}
 2. \text{ Torque Ripple} &= (\text{max peak torque} - \text{min peak torque}) \\
 &= 8.7-6 \\
 &= 2.7 \text{Nm}
 \end{aligned}$$

Torque ripple as shown in simulation output is 2.6204 Nm

Theoretically calculated value:

$$\begin{aligned}\% \text{ Torque ripple} &= (\text{max peak torque} - \text{min peak torque})/\text{average torque} \\ &= (8.7-6.0)/7.35 \\ &= 36.7\end{aligned}$$

Software output:

$$\begin{aligned}\% \text{Torque ripple} &= (\text{max peak torque} - \text{min peak torque})/\text{average torque} \\ &= (2.2604)/7.4052 \\ &= 35.30\end{aligned}$$

6.9 GRAPHS

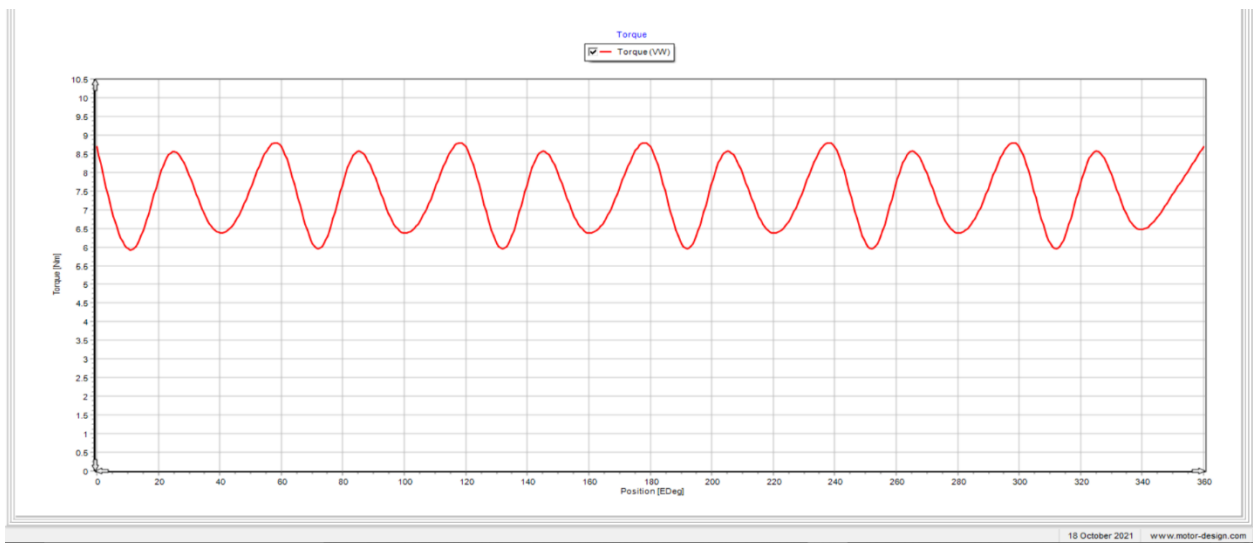


Figure 42: Torque vs Position

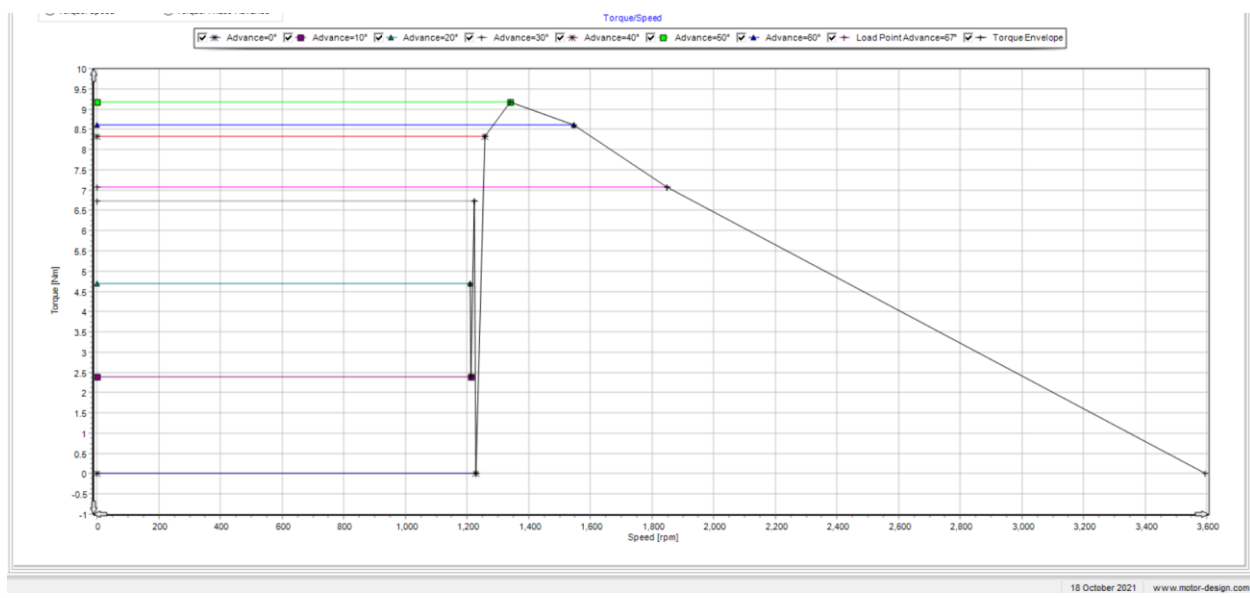


Figure 43: Torque vs Speed

6.10 E -MAGNETICS

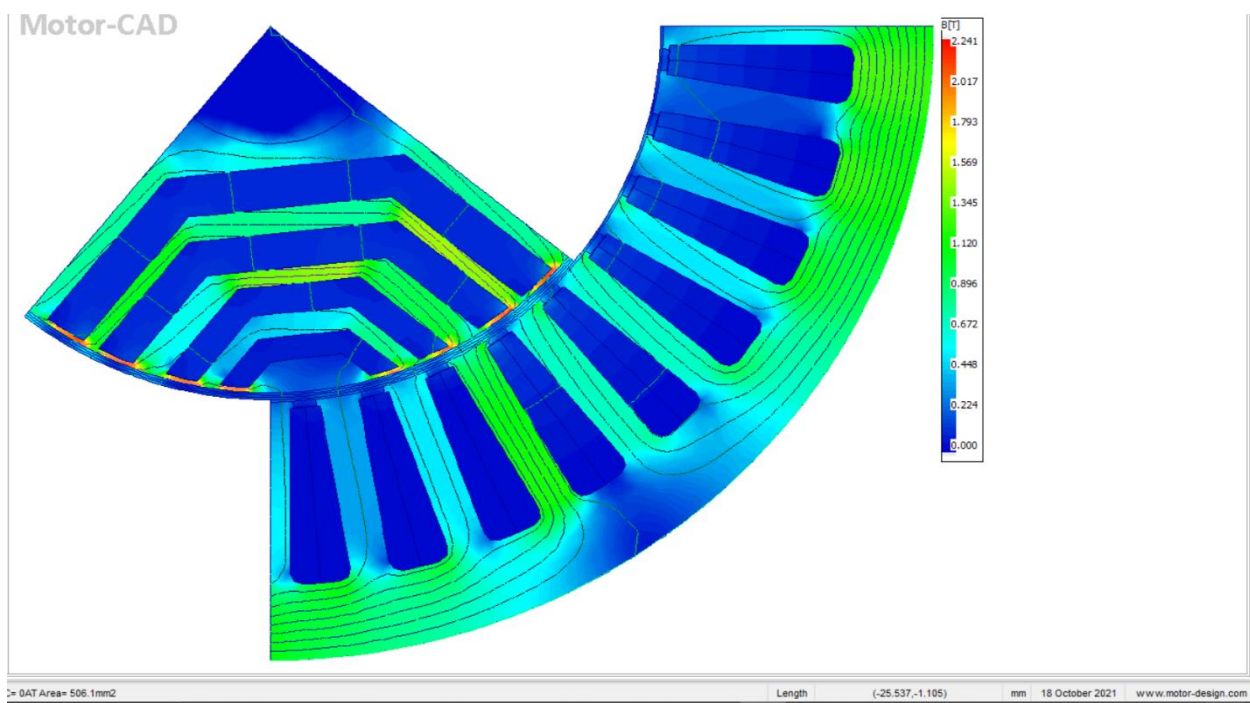


Figure 44: E-Magnetics for 4 Flux Barrier Model

7

ANALYSIS AND VERIFICATION

7.1 ROTOR DESIGN CHARACTERISTICS

The rotor of a speed controlled SynRM should be designed with Saliency ratio as large as possible. In other word the d axis inductance (L_d) should be higher than the Q-axis inductance (L_q).

The saliency ratio also largely determines the characteristics of the SynRM that is what the peak torque of the machine is, how fast the machine responds to the dynamic change occurrence and what power factor and efficiency can be reached. To be competitive with the induction machine of the same size saliency ratio must be in the range of 6 to 10.

The saliency ratio of the SynRM with conventional salient pole configuration is too low for it to compete with induction motor equipped with a similar stator.

The (L_d/L_q) ratio must be as high as possible to achieve maximum torque and saliency ratio must be large to achieve maximum power factor.

7.2 SALIENCY RATIO

$$\text{Saliency ratio} = (L_d/L_q)$$

Where

L_d is D -axis Inductance in mH

L_q is Q-axis Inductance in mH

Saliency ratio is defined as the ratio of d axis inductance to q axis inductance.

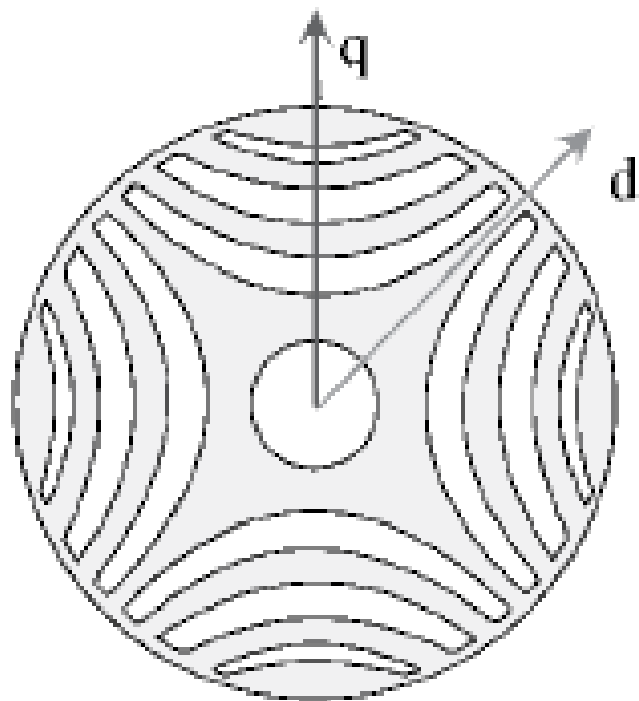


Figure 45: D and Q Axis

7.3 SYNRM WITH 1 AND 2 FLUX BARRIERS

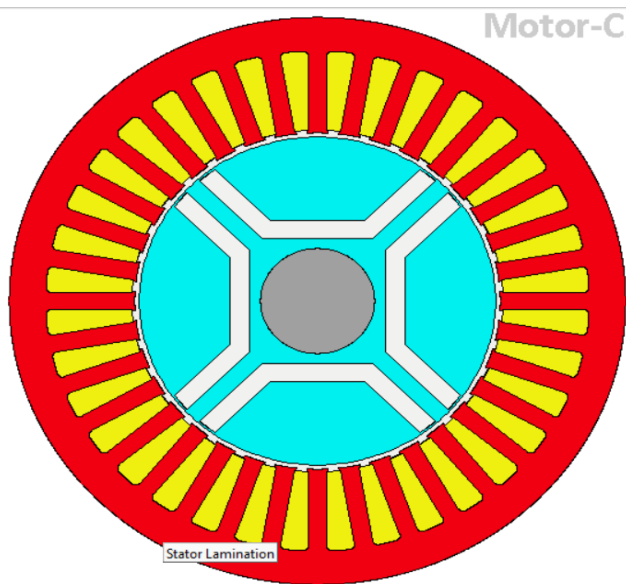


Figure 46: SynRM with 1 flux barrier

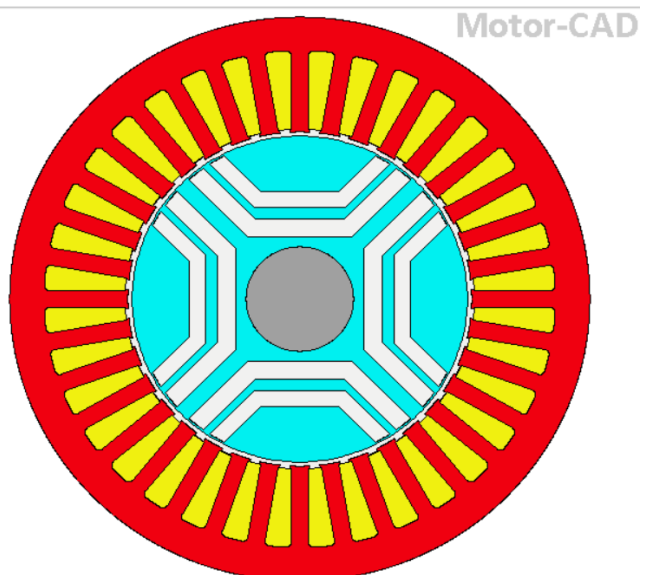


Figure 47: SynRM with 2 flux barrier

7.4 OUTPUT AND INFERENCE

| PARAMETER | 1 FLUX BARRIER MODEL | 7 FLUX BARRIER MODEL |
|-----------------------|----------------------|----------------------|
| D AXIS INDUCTANCE(MH) | 300.2 | 302.2 |
| Q-AXIS INDUCTANCE(mH) | 128 | 90.55 |
| (Ld-Lq) | 172.2 | 211.65 |
| Saliency ratio | 2.34 | 3.3 |

Table 2: Saliency Ratio

Where

Ld- D-axis Inductance in mH

Lq – Q-axis Inductance in mH

(Ld-LQ) ratio

Ld/Lq- Saliency ratio

The torque production capability of the synchronous reluctance machine is generally related the (Ld-Lq) ratio higher the ratio greater is the torque production. Similarly, if Saliency ratio is high the power factor of the machine can be increased. As in 1 and 2 flux barrier model the saliency ratio is low so we need to move to 3 or 4 flux barrier model to improve saliency ratio.

7.5 MULTILAYER BARRIER MODEL

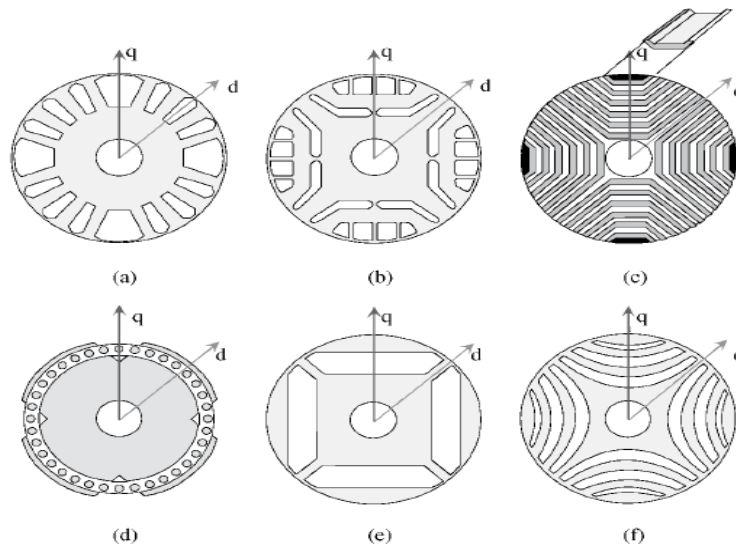


Figure 48: Multilayer Barrier Model

The geometry shown is figure (c) produces the largest saliency ratio. Its laminations are axially oriented but they are stacked in the radial direction. The (L_d/L_q) values for this rotor geometry are normally greater than 10 and might exceed even 15. However, figure 1.2a shows a model with multilayer flux barrier its saliency ratio is lower because of the rotor supporting steel parts in the round laminations .in multilayer flux barrier rotor model the several stack sections are first cut away from the rotor palate when assembling the rotor stack, these sections are can be filed with desired non-magnetic materials via dicasting. This way construction of the model becomes quite stronger. The ratio of the conductor to insulation layer can affect the saliency ratio of the machine.

When the proportion of the iron layer increases the ratio of the iron thickness along with the area of the cross section of the magnetic circuit part of the d axis flux also increases. And therefore, the L_d increases. However, as the insulation size becomes thinner the preventive layer on the progression of the flux diminishes and q axis inductance decreases. Beyond 10 layers the total no of insulation and conductor layers do not significantly affect the saliency ratio.

7.6 RESULTS IN 3 AND 4 BARRIER MODEL

| PARAMETER | 3 FLUX BARRIER MODEL | 4 FLUX BARRIER MODEL |
|------------------------|----------------------|----------------------|
| D axis inductance(mh) | 300.6 | 302.1 |
| Q-axis inductance (mh) | 77.32 | 73.2 |
| (Ld-Lq) | 223.8 | 230.9 |
| Saliency ratio | 3.88 | 4.11 |

Table 3: Saliency Ratio for 4 flux barrier

7.7 NEED FOR FLUX BARRIERS AND CARRIERS

Unlike Induction machine SynRM rotor design requires saliency of the poles to provide comparable performance to the IM. The Direct axis (q-axis) is where there is more iron in the circuit the phase will measure high open circuit inductance. Through the Direct axis, the flow will be higher.

In Quadrature axis the air passages block the flow of flux.

7.8 RELATION BETWEEN POWER FACTOR AND NO OF FLUX BARRIERS

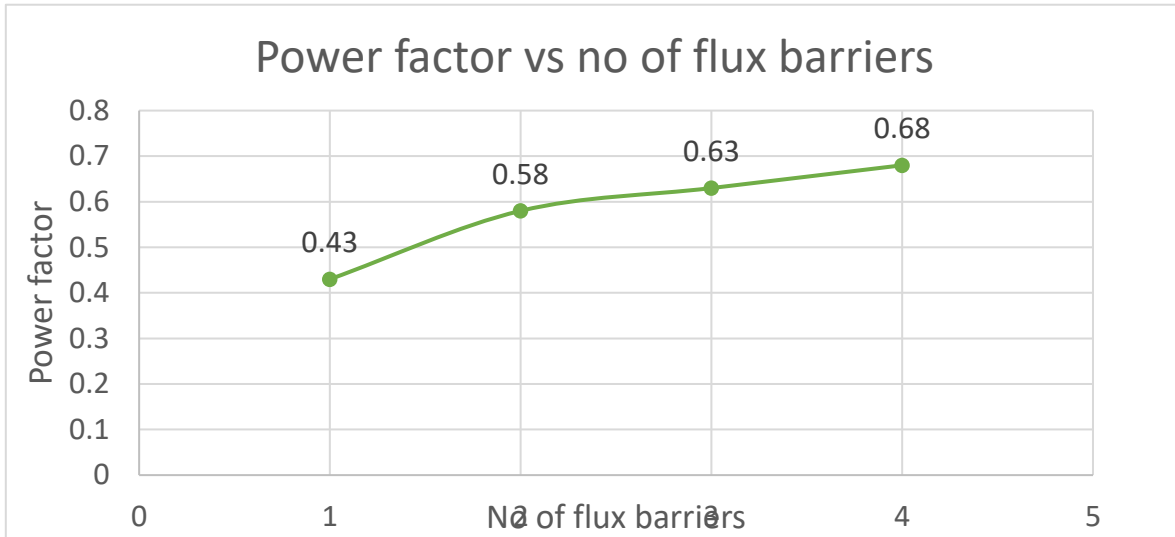


Figure 49: Power factor vs No. of Flux Barriers

With increase in no of flux barriers the power factor obtained is higher. SynRM with 4 flux barriers has the highest power factor noted.

7.9 RELATION BETWEEN SALIENCY RATIO AND NO OF FLUX BARRIERS

By modelling SynRM with different no of flux barriers, the saliency ratio is noted to higher for the SynRm with 4 flux barriers.

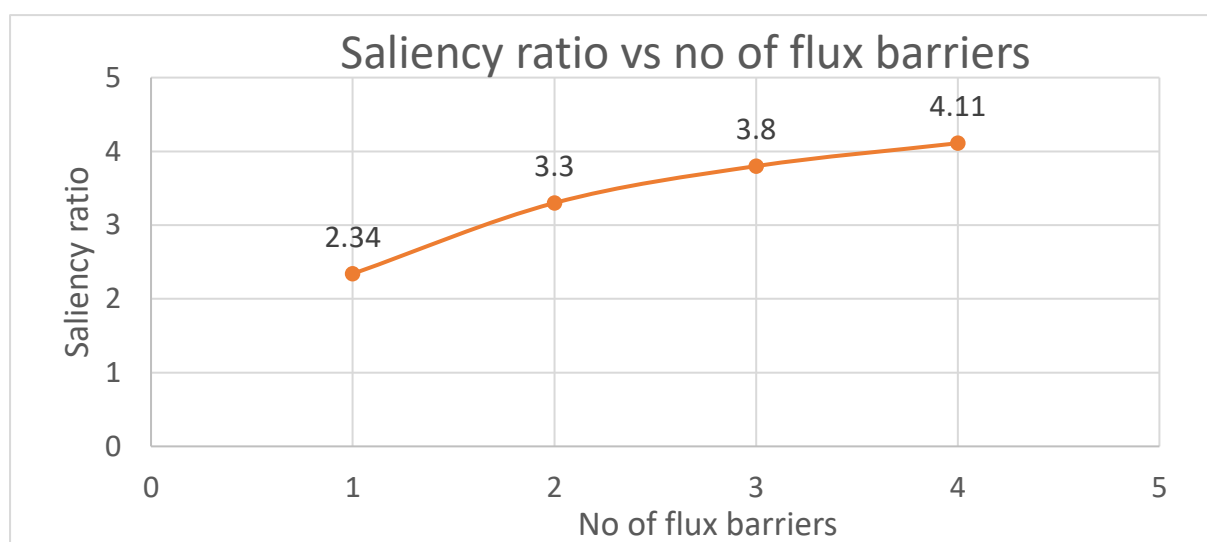


Figure 50: Saliency ratio vs No. of Flux Barriers

7.10 REALTION BETWEEN SALIENCY RATIO AND POWER FACTOR

In SynRM the value of the inductances on the two axes play a major role and are very important due to the fact that torque is directly related to the difference between them and while maximum power factor is dependent on their ratio.

$$Pf = ((Ld/Lq) - 1) / ((Ld/Lq) + 1)$$

$$\text{Torque} = m * p * I_d * I_q * (L_d - L_q)$$

Where, m is the number of phases, p is no of poles and id and iq are d axis current and q axis current.

7.11 RELATION TO ACHIEVE MAXMIMUM POWER FACTOR

The power factor reaches its maximum at this current angle

$$k = \arctan(\sqrt{(L_d/L_q)})$$

where,

L_d = d axis inductance mH

L_q = Q axis inductance mH

L_d/L_q is saliency ratio of the machine.

K is the current angle for SynRM

7.12 RESULTS FOR 3 FLUX BARRIER MODEL

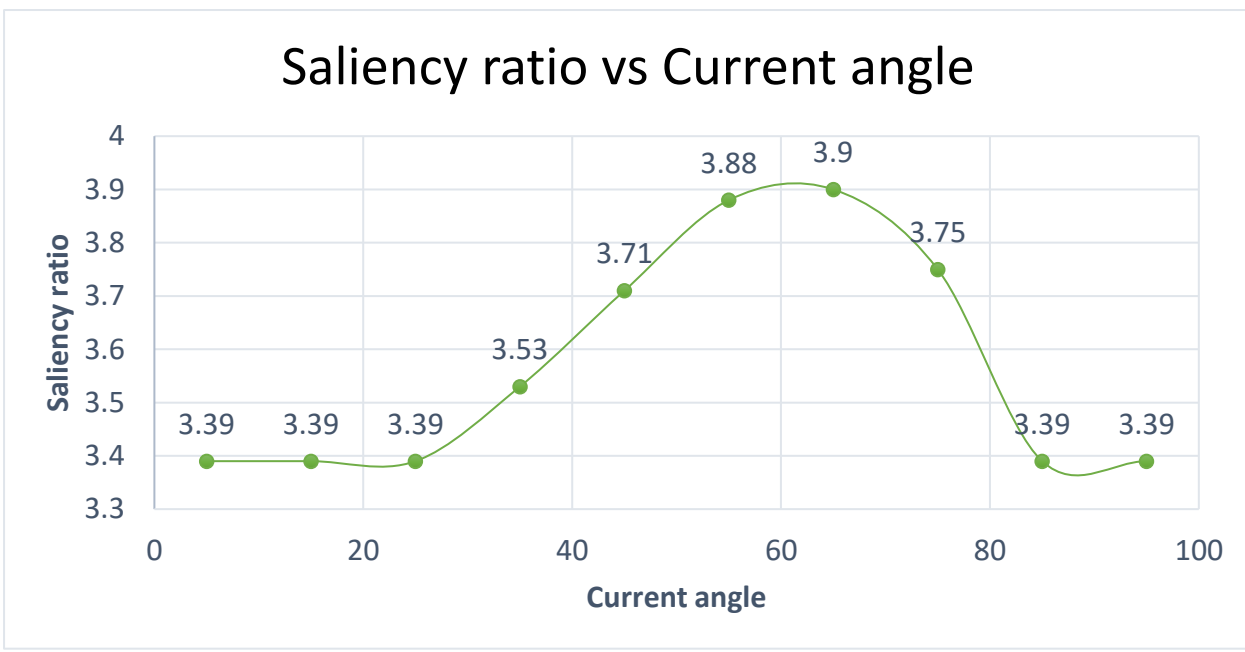


Figure 51: Saliency ratio vs Current angle

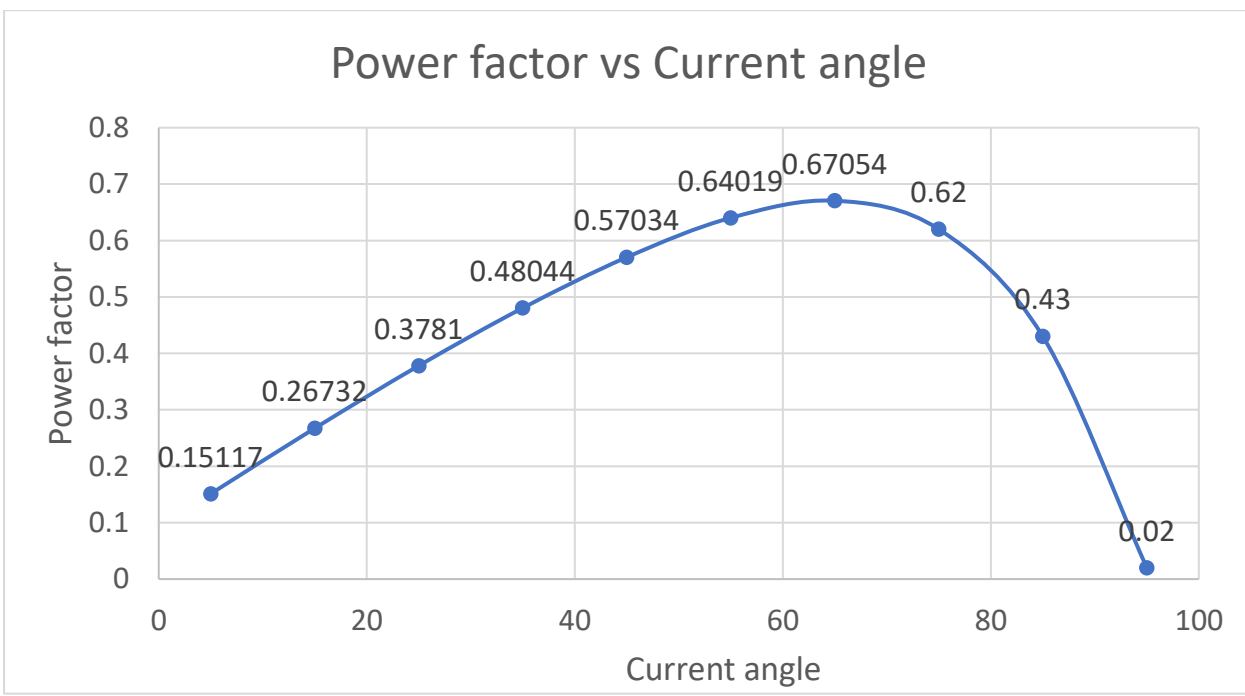


Figure 52: power factor vs current angle

By varying the current angle by 5 deg the changes in the power factor and saliency ratio can be noted. The maximum power factor is achieved at an angle of 65 deg for the 3 flux barrier model where the saliency ratio is also max for 65 degree current angle, however the torque ripple obtained is higher in 3 flux barrier model. So, we move on to 4 flux barrier model.

7.13 TO ACHIEVE MAXIMUM POWER FACTOR

In our case to achieve maximum power factor we take the maximum saliency ratio value attainable.

Say for $L_d/L_q=4.11$ (For 4 flux barrier model)

$$\text{Current angle, } k = \arctan(\sqrt{4.11})$$

$$= 64^\circ$$

For this current angle from the graph we can note that the power factor obtained is 0.68 which is the maximum power factor obtained. Similarly, if the current angle is known necessary saliency ratio to attain high pf can be obtained. We can also note that at this current angle the torque ripple attained is also low.

7.14 RESULTS OBTAINED FOR 4 FLUX BARRIER MODEL

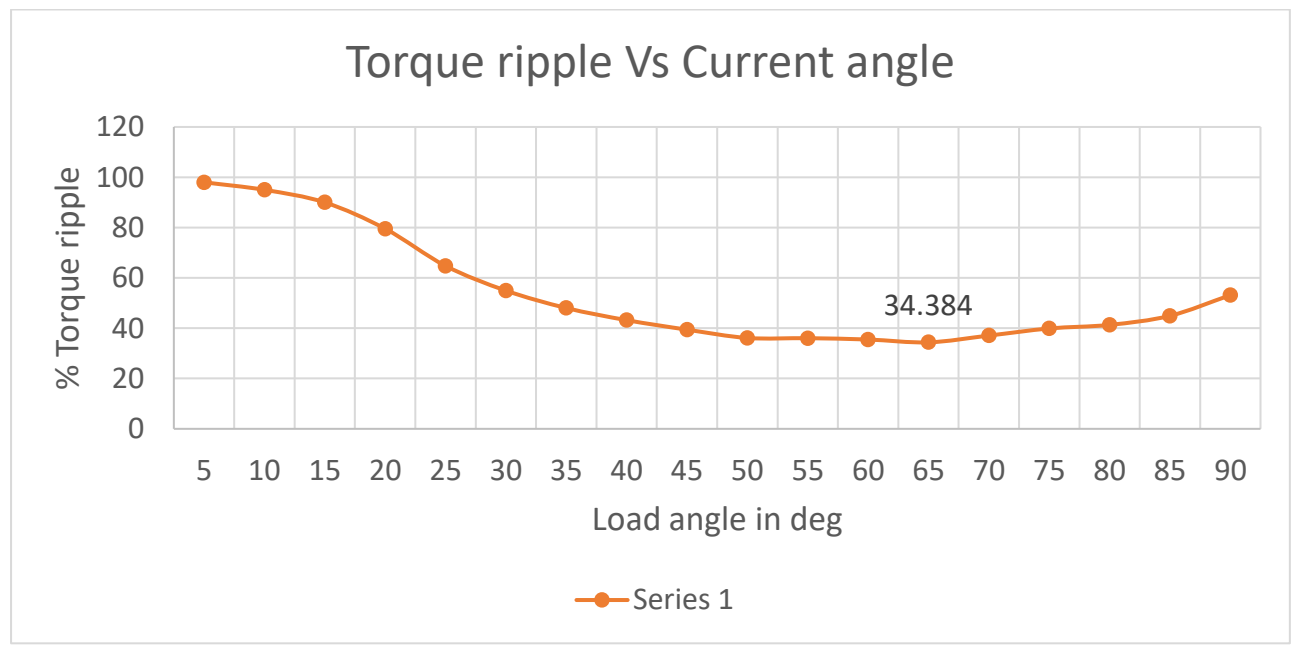


Figure 53: Torque ripple vs Current angle

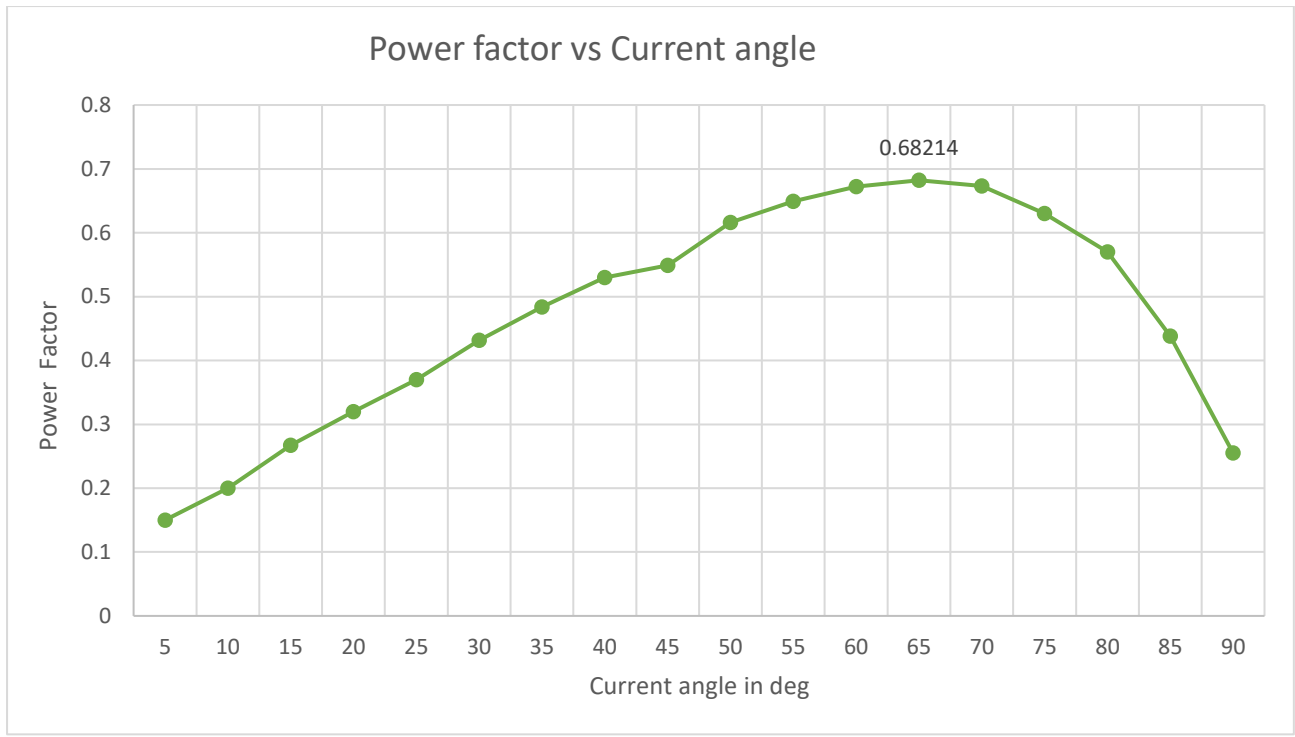


Figure 54: power factor vs current angle

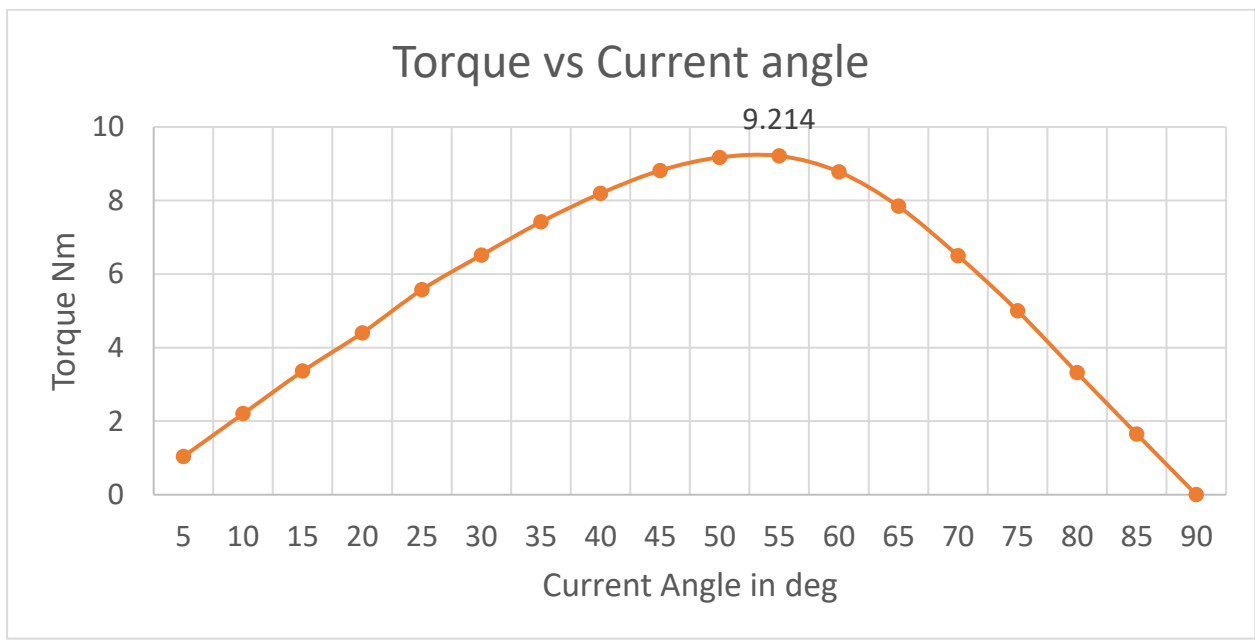


Figure 55: Torque vs Current angle

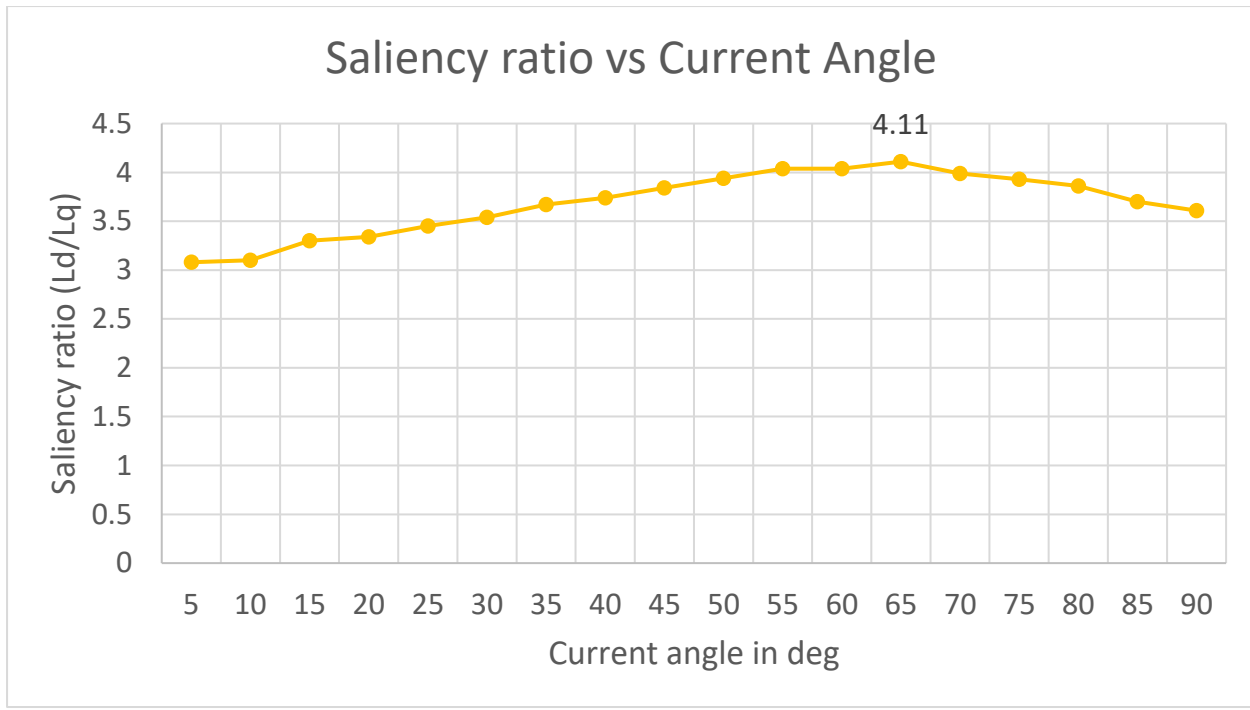


Figure 56: saliency ratio vs current angle

8

COMPARISON BETWEEN IM AND SYNRM

| PARAMETERS (Units) | INDUCTION MACHINE | 3 FLUX BARRIER SYNRM | 4 FLUX BARRIER SYNRM |
|--|----------------------|----------------------------|----------------------------|
| No of Phases | 3 | 3 | 3 |
| Frame | 90L | 90L | 90L |
| Duty | S1 | S1 | S1 |
| Insulation Class | F | F | F |
| Frequency (Hz) | 50 | 50 | 50 |
| IP | 55 | 55 | 55 |
| Weight (Kg) | 21.0 | 18.0 | 18.0 |
| TR (degree Celsius) | 70 | 40 | 40 |
| No of Poles | 4 | 4 | 4 |
| Input Power (KW) | 2.65 | 2.65 | 2.65 |
| Speed (RPM) | 2876 | 3000 | 3000 |
| Armature Current (A) | 4.8 | 5.5 | 5.5 |
| Output Power (KW) | 2.2 | 2.2 | 2.2 |
| Shaft Torque (Nm) | 7.64 | 7.24 | 7.30 |
| Power Factor | 0.75 | 0.65 | 0.68 |
| Efficiency (%) | 83.23 | 86.50 | 86.72 |
| Torque Ripple Percentage | - | 41 | 35.4 |
| Saliency Ratio (at 65degree current angle) | - | 3.88 | 4.11 |

Table 4: Comparison between IM and SynRM

9

CONCLUSION

An induction motor with rating of 2.2kW and Synchronous reluctance motor with rating of 2.2kW was modelled using ANSYS MotorCAD.

9.1 SUMMARY OF WORK DONE

The induction motor and Synchronous Reluctance motor name plate details were obtained from DANFOSS LAB FOR CLIMATE TECHNOLOGY and they were modelled for a rating of 2.2kW, 4 pole with 3000 rpm using ANSYS MotorCAD.

SynRM rotor for 4 different models (1 flux barrier, 2 flux barrier ,3 flux barrier, 4 flux barrier) were modelled and the torque, torque ripple and power factor for the following models were inferred.

To obtain maximum power factor SynRM with 3 and 4 flux barrier models were compared and with the variation of current angle and saliency ratio and power factor of the 4 flux barrier machine were found to be improved and it was better than the results obtained for 3 flux barrier model.

The 3 flux barrier model resulted in 41.4% torque ripple however 4 flux barrier model produced 35.3% torque ripple.

9.2 FUTURE WORK

In future we have planned to analyse PMSynRM (permanent magnet assisted SynRM) with different magnet materials and by changing position or arrangement of magnets. SynRM with and without permanent magnets will be compared. we have planned to analyse which one would be suited for electric vehicles as a replacement for PMSM

BIBLIOGRAPHY:

1. Duc-Kien Ngo, Min-Fu Hsieh. Performance Analysis of Synchronous Reluctance Motor with Limited Amount of Permanent Magnet, Energies.
2. Hui Yu, Xinxing Zhang, Jinghua Ji, Liang Xu. Rotor Design to Improve Torque Capability in Synchronous Reluctance Motor, IEEE.
3. S. Tahi, R. Ibtiouen, M. Boumekhla. Design Optimization of Two Synchronous Reluctance Machine Structures with maximised Torque and Power Factor, Journal progress in Electromagnetic Research B35.
4. Alireza Siadatan, Jacob Goltieb, Ebrahim Afjei. Comparison of power factor between permanent magnet assisted synchronous reluctance motor with neodymium-iron-boron and ferrite magnets, IEEE.
5. Nezih Gokhan Ozcelik, Ugur Emre Dogru, Murat Imeryuz and Lale T. Ergene. Synchronous Reluctance Motor vs Induction Motor at low power Industrial Applications: Design and Comparison, Energies.
6. Sibasish Panda, Ritesh Kumar Keshri. Design and Analysis of Synchronous Reluctance Motor for Light Electric Vehicle Application, IEEE.
7. Andre Nasr, Baptiste Chareyron, Abdelli Abdenour and Misa Milosavljevic. Design of a Permanent Magnet assisted Synchronous Reluctance motor using Ferrites, IEEE.
8. Gianmario Pellegrino, Thomas M. Jahns, Nicola Bianchi, Wen L. Soong, Francesco Cupertino. The Rediscovery of Synchronous Reluctance and Ferrite Permanent Magnet Motors, Springer.
9. Olexiy Iegorov, Olga Iegorova, Mykolay Kundenko, Natalia Potryvaieva. Ripple Torque Synchronous Reluctance Motor with Different Rotor Designs, IEEE.

10. Ken Chen, Wenfei Yu, and Chuanxin Wen. Rotor Optimization for Synchronous Reluctance Motors, IEEE.